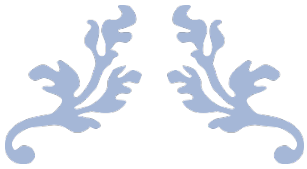

REMOVAL OF CR(VI) IN WASTEWATER BY MN/AL-LDH AND ITS MODIFIED MATERIALS

Chengrui Xie, MEng

THESIS SUBMITTED TO THE UNIVERSITY OF NOTTINGHAM FOR THE DEGREE OF MASTER OF RESEARCH

Abstract

With the rapid development of industrialization in modern society, the excessive discharge of industrial wastewater containing chromium ions generated during industrial production has caused serious environmental pollution. In particular, Cr^{6+} is extremely toxic and cannot be easily removed by degradation after entering the environment. And it will accumulate and accumulate in the environment for a long time, poisoning organisms and human bodies through the food chain.

At present, there are many methods for treating heavy metal-containing wastewater. The common main methods are: adsorption method, biological method, membrane separation method, chemical precipitation method and electrochemical method. Among them, the adsorption method has been widely studied and applied due to low cost and high removal rate. Common adsorbents are activated carbon, chitosan, chelate resin, and clay minerals. Clay minerals have attracted more attention and research due to its high removal rate, environmental friendliness and reusability.

LDH (Layered double hydroxide) material is a typical anionic layered clay mineral. However, traditional LDH materials can only remove chromium ions through adsorption, but cannot reduce Cr^{6+} to less toxic Cr^{3+}, and do not really remove the harm of Cr^{6+}. In order to solve this problem, in this paper, a fixed ratio (Mn: Al = 2: 1) Mn/Al-LDH material was prepared by hydrothermal synthesis. At the same time, it was tried to be modified with zeolite to form a new Zeolite-Mn/Al-LDH material with higher specific surface area. At the same time, XRD, SEM, TEM and BET characterization and analysis were performed on these two materials before the adsorption reaction. The research showed that the prepared LDH had a complete

crystal structure, good crystallinity, and small crystal particles. By BET characterization, it has been observed that that the BET surface area values of Zeolite-Mn-Al-LDH and Mn-Al-LDH are 47.49 ± 0.11 m^2/g and 33.41 ± 0.17 m^2/g. Then, the removal of Cr^{6+} from simulated wastewater by these two LDH materials was studied. It was observed during experiment that the modified Zeolite-Mn-Al-LDH can adsorb Cr^{6+} ion in solution faster than ordinary Mn-Al-LDH. When the reaction time reaches 90 min, the removal efficiencies of the two LDH are both close to 98%, respectively, which means that both two LDH can effectively remove Cr^{6+} in sufficient time. By comparing with past researches, it is speculated that the removal process involves the simultaneous effects of adsorption, reduction, and co-precipitation. On the one hand, hexavalent chromium is fixed to the interlayer and surface of LDH by interlayer ion exchange adsorption or surface adsorption. Subsequently, Mn^{2+} on the laminate will reduce Cr^{6+} to Cr^{3+}. At the same time, Mn^{2+} will be oxidized to high-valent Mn ions, and co-precipitate with chromium in solution.

Keywords: Cr^{6+}, Cr^{3+}, layered double hydroxides, removal

Publications

Yu Hong, **Chengrui Xie**, Wanru Chen, Xiang Luo, Kaiqi Shi, Tao Wu, (2019) Kinetic study of the pyrolysis of microalgae under nitrogen and CO2 atmosphere, Renewable Energy, 145 (2020), p:2159-2168.

Courses attended

1. Laboratory Safety Training (UNNC)
2. An Introduction to Writing for Academic Journals (UK) (18-19)
3. Literature Searching and the Literature Review (UK) (18-19)
4. Effective Literature Searching
5. Understanding Supervision
6. Planning Your Research
7. Research Data Management

Acknowledgement

I would like to express my sincere appreciations and gratitude to Professor Tao Wu and Dr. Xiang Luo for their invaluable guidance and support throughout the period of my MRes period. Working with them provided an enriching experience to my academic life at the University of Nottingham, Ningbo, China. Their encouragement and support were instrumental in the completion of my thesis.

I would like also to express my thanks to the staff members who helped and gave me precious suggestions in research work and experiments, especially Dr. Kaiqi Shi, Dr. Xiang Luo, Carey Tao, Gang Yang, Kelly Yao, Karen Ning, Jessica Wang, Julian Zhu, Jane Zhang, Karey Shan, Helen Xu etc. I also appreciate the help and support from all my colleagues and friends: Dr. Yipei Chen, Dr. Yu Hong, Dr. Luyao Tang, Yuxin Yan, Xueliang Mu, Shuai Liu, Peng Jiang, Jiahui Yu, Fengjuan Song, Dr. Shu Liu, Dr. Huayang Li, Jinwei Cao, Yiming Yin, etc.

Contents

Chapter 1 Background of Cr^{6+}

1.1 Overview

With the continuous economic and social development, the utilization of heavy metal resources has increased rapidly. At the same time, a large amount of heavy metal-polluted industrial wastewater and solid waste are produced in chemical production and other industrial production processes. The main sources of industrial wastewater containing heavy metals are electroplating electrolysis industrial activities such as metal products, paints and dyes production[1-3]. Heavy metals may eventually accumulate in food chains and water cycle and finally endanger human health [4, 5]. Normally, natural water or soil environments have very limited ability to deal with heavy metal pollutants by biodegradation. At the same time, some heavy metals ions, such as Cr^{6+}, can be converted to highly toxic compounds by the action of microorganisms. Therefore, With the increasingly serious water pollution by heavy metal, heavy metal wastewater treatment has become imminent[6].

Apart from causing environmental pollution and ecological damage, heavy metals also cause great health hazards to the human body. Taking chromium (Cr) as an instance, which is considered as a powerful hazard to both nature and humans[11, 12]. Chromium exists mainly in the form of Cr^{3+} and Cr^{6+} in the natural environment. Among them, a certain amount of trivalent chromium plays a role in the metabolism of sugar and cholesterol in human body's metabolism. Nonetheless, excessive Cr^{3+} in the human body will cause damage to human health. Cr^{6+} is the most toxic in all valence chromium ions, and its toxicity is more than 100 times higher than trivalent chromium[13, 14]. It is studied that the main sources of Cr^{6+}-

containing wastewater include leather industries, textile and metal finishing, electroplating industries and tanning[15]. Due to the wide applications of Cr^{6+} in the industry, the pollution of it to natural environment is becoming increasingly serious, which brings great harm to the natural environment on which people depend for survival and the human being itself.

The main damage caused by Cr^{6+} can be listed based on two categories. First of all, Cr^{6+} is a threat to the environment. Specifically, a certain amount of Cr^{6+} can change the color of the water. When the concentration of chromium in the water reaches 1 mg/L, the chemical properties of the water will change. In addition, chromium can also accumulate in plants by means of bioaccumulation, which finally harms human health through the food chain. This leads to the second hazard of Cr^{6+}: an enormous threat to human health. Chromium poisoning in human body is mostly caused by Cr^{6+}. Cr^{6+} is able to invade into human body through atmosphere, water and food, leading to skin erosion, respiratory infection, and even cancer. After entering human body, Cr^{6+} constitutes a compound with a ligand such as phosphate, methionine or serine in the living body, thereby destroying the catalysis function of the enzyme. Cr^{6+} is reduced to trivalent in red blood cells, which inhibits the activity of gluten reductase and simultaneously converts hemoglobin into methemoglobin. This will lead to serious interference in the REDOX and hydrolysis processes[16-19]. Moreover, Cr^{6+} has obvious carcinogenic effects, and it is a certain carcinogen published by the International Agency for Research on Cancer (IARC). Therefore, research on the treatment and reuse of chromium-containing wastewater has become one of the important environmental problems faced by humanity. According to United States Environmental Protection Agency (US-EPA), the maximum contaminant level (MCL) for Cr was 0.1 ppm in

drinking water[20]. Based on the novel Integrated Wastewater Discharge Standard published in 2019, the maximum allowable emission concentration (mg/L) of Cr and Cr^{6+} are showed as Table 1-1. Wastewater under this standard is defined as water that is emitted during industrial production and human daily life.

Table 1-1. The maximum allowable emission concentration (mg/L) of Cr and Cr^{6+} in 2019.

Pollutants	Maximum allowable emission concentration (mg/L)
Total chromium (Cr)	1.5
Hexavalent chromium (Cr^{6+})	0.5

Among all heavy metal pollutants, due to the large amount of chromium-containing pollutants produced by extensive industrial production, chromium pollution has attracted increasing attentions by researchers. On the other hand, the existing heavy metal treatment methods such as chemical, biological, electrolysis, and membrane all have their limitations. The LDH (Layered Double Hydroxides), as a natural clay mineral material, has the properties and ability to remove contaminants from water bodies due to its special layered structure controllability and interlayer anion exchangeability [20, 21]. Therefore, the application of LDH materials to the removal of heavy metal ions can be considered.

1.2. Research Objectives

The significance of this study is to synthesize a LDH material based on the removal mechanism to remove Cr^{6+} in water, so as to reduce the harm of heavy metal Cr^{6+}. On this basis, the LDH are modified to improve the material. Reducing and adsorbing properties of hexavalent chromium to

achieve efficient treatment of heavy metal contaminants.

Based on previous researches, chromium electroplating and anodizing tanks are recognized as the largest sources of chromium emissions in the US Cr^{6+}, which is highly toxic and a confirmed carcinogen. Breathing numerous of hexavalent chromium can harm and irritate nose, lungs, stomach, and intestine[22]. Therefore, the main work of this paper includes the synthesis and characterization of traditional Mn/Al-LDH and modified Zeolite-Mn/Al-LDH materials. Then, these two types of LDH materials are characterized by XRD, SEM, TEM and BET, respectively, in order to firstly determine the chemical composition of the material, and then recognize the chemical structure and morphology of these two LDH materials. Formerly, two different LDH materials are applied to test the adsorption ability of Cr^{6+} in wastewater and the results are going to be compared and analyzed.

Chapter 2 Literature review

2.1 Heavy metal pollution control

Due to the bioenrichment and difficult to biodegradation, heavy metal water pollution is difficult to treat by conventional technology in sewage treatment plants. At present, researchers have conducted numerous researches on heavy metal water pollution. The methodologies most related to this study include chemical method and adsorption method [23].

2.1.1 Chemical method

Chemical treatment method of heavy metal pollution mainly includes chemical precipitation method, redox method and ferrite precipitation method.

Based on principles of solubility product, the basic steps of the chemical precipitation method for treating heavy metal wastewater are: putting a specific chemical precipitant into the pending wastewater and producing a chemical precipitation reaction. Then, the precipitation of heavy metal ions in the wastewater is processed and the precipitate can be removed by a solid-liquid separation step. The chemical reaction that produces precipitation mainly includes metathesis reaction and complexation reaction. The main methods are as follows: the first is through adding chemical reagents to produce the corresponding reaction between heavy metal ions and chemical reagent and thereby form an insoluble precipitate. Second, adjusting the pH of the solution by an acid reagent or an alkali reagent, making it possible for heavy metal ions to form sulfides, hydroxides and

other precipitates. Due to the simplicity of process technology, convenience of operation technology and low cost of processes, chemical precipitation method has been widely applied in the field of heavy metal wastewater treatment. However, the disadvantages of the chemical precipitation method are also significant: industrial equipment of treatment needs a large area and chemical reagent consumption is definitely high. Moreover, the generated precipitate can only be easily buried and difficult to carry out subsequent treatment, which is easy to produce secondary pollution[23-25].

Redox method has been widely used in the treatment of heavy metal wastewater. Its main advantages include low operating and maintenance costs, significant effect of sewage treatment and convenient operation processes. The key to this method is to choose the right oxidant and reducing agent[26]. As to ferrite precipitation method, it is a new type of chemical treatment method for treating wastewater containing heavy metal ions, which was first proposed by the Japanese Electric Company. The basic principle is to achieve the purpose of wastewater purification under alkaline conditions[27, 28]. Hu et al.[29] applied $Ca(OH)_2$ to remove mercury from wastewater. According to the results, under the condition of pH value was 8, the dosage was 1 time and the reaction time was 10 min, the result of treatment effect showed that the Hg^{2+} decreased from 0.1 $mg \cdot L^{-1}$ to 0.04 $mg \cdot L^{-1}$, which was lower than the limit in the national emission standard. In addition, the three heavy metal ions of Cd^{2+}, Pb^{2+} and Cu^{2+} have an inhibitory effect on the removal of Hg^{2+} by $Ca(OH)^2$, and the influence order is $Cu^{2+}>Pb^{2+}>Cd^{2+}$, and Zn^{2+} promotes the process.

2.1.2 Adsorption method

Adsorption method is a methodology for adsorbing and heavy metal pollutants treating heavy metals problems in wastewater by using porous adsorbent materials, which is recognized as a relatively mature and simple wastewater treatment technology. This category of technology has simple operation process and the adsorption materials can be recycled. In recent years, engineers and researchers are more inclined to find a more suitable cheap adsorbent material to support industrial adsorption work. The adsorbent plays a key role in the adsorption treatment process. Generally, a porous material having a large specific surface area is selected as the adsorbent material. On this premise, industrial adsorbents must have the characteristics of strong adsorption capacity, low adsorption equilibrium concentration, good mechanical strength, low price and easy to be regenerated.[30-32]

There are many methods for treating heavy metal-containing wastewater, while different methodologies have their limits. Among them, the biological treatment of heavy metal-containing wastewater is greatly affected by the external environment. Additionally, on account of the complexity of the biological cell itself and the slower reproduction rate, biological treatment method has not been widely used in industrial wastewater treatment[32-35].In addition to biological treatment method, the problem of chemical precipitation method in the treatment of heavy metal wastewater is a manifestation of the large demand for reagents and high energy consumption[36, 37]. Besides, as the point mentioned previously, electrochemical methods are not suitable for treating low concentration wastewater[38-40]. As to membrane separation method, this process shows a high energy conversion rate and separation efficiency when

treating chromium-containing wastewater. And the equipment of membrane device is relatively simple and easy to operate, which makes this technology have broad application prospects in the field of wastewater treatment. However, the shortcoming of this method is that industrial wastewater often contains impurities such as acid, alkali, oil and other substances, making the treatment conditions of its wastewater more rigorous[41-43]. Lin [44]attempted to load nano-Fe_3O_4 particles with Aeromonas, on the basis of maintaining the excellent magnetic responsiveness and biocompatibility of Fe_3O_4, the problem of insufficient surface coordination is solved, and a new adsorbent with higher removal efficiency is obtained. The experimental results showed that after 60 minutes of reaction time, the adsorption efficiency of the lead ions can reach 89.93% by adding 0.5 g/L of the adsorbent at a concentration of 30 mg/L of lead ion and maintaining the pH of the solution for 4.

Compared to other treatment approaches, adsorption method has been widely studied and applied due to the low price of the materials used and the splendid treatment effect. Common adsorbents include activated carbon[45, 46], chitosan[47], chelate resin[48, 49] and clay minerals. Among them, clay minerals have attracted more attention because of their high removal rate, environmental friendliness and reusability. Layered double hydroxides (LDH) material is a typical anionic layered clay mineral, but traditional LDH materials can only remove chromium ions by adsorption. This method is only a transfer of pollutants. It cannot reduce hexavalent chromium to trivalent chromium which is less toxic, and does not really remove the hazard of hexavalent chromium. Therefore, this research aims to develop a LDH material based on the reduction-adsorption mechanism to reduce the toxicity of hexavalent chromium.

2.2 LDH materials overview

LDH is a category of double-layered hydrated metal oxide, including LDH compounds and LDH-like compounds, the body of which is generally composed of two types of metal hydroxide oxides. By measuring its single crystal structure, it is determined that its structure is similar to the regular octahedral structure of brucite. While considering the existing targets of synthesis and applications in laboratory scale, for instance, catalysis, biomedicine, energy saving and waste disposal, LDH have a high potential for industrial applications. In order to enhance the industrial application value of LDH, accessible production of particles in a steady morphology is necessary. This means the mean size and distribution of particles are required to be controlled, and aspect ratio as well as particle shape is also operated in a unified standard. After controlling the properties of LDH in morphological scale, it is proved that LDH has been wildly applied to multiple fields, including adsorbents [50], support and precursor of catalysts [51, 52], as well as fire retardant [53]. Moreover, in the field of environmental remediation [54] and catalysis [55], nanohybrids-based LDH and nanocomposites-based LDH have proved to have a wider potential then the materials with normal morphology.

2.2.1 Structures

Naturally, LDH is able to be recognized as two polymorphic forms, namely rhombohedral and hexagonal, which are respectively showed as in Figure 2-1.

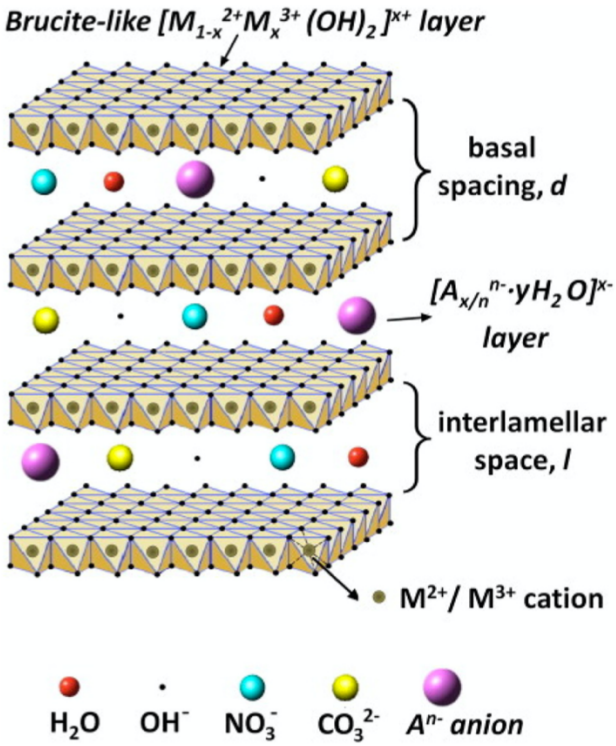

Fig. 2-1. Schematic representation of the LDH structure

LDH materials are acknowledged as one type of bidimensional materials which attract rising attention because of their composition diversity and various applications. In addition to this, LDH are recognized as anionic clays or compounds with LDH-like structure, which can be described by the typical formula

$$[M(II)_{1-x}M(III)_x(OH)_2][(A^{n-})_{\frac{x}{n}}.mH_2O]$$

Where, M[II] and M(III) are divalent and trivalent cations, A^{n-} is a charge compensating interlayer anion, m the number of water molecules and x the molar fraction of trivalent cations ($0.2 < x < 0.4$).

Compared to LDH layer structure, the structure of $Mg(OH)_2$ can be considered as the similar template. This means both these two types of structures have edge-sharing octahedra of divalent cations in the central site, which are surrounded by six single hydroxyl groups and give rise to

abundant sheets. Additionally, various divalent cations in the LDH structure can be isomorphically substituted by trivalent cations, which means divalent cations in LDH tend to be replaced by cations with higher charge and moderately similar ionic size. The brucite-like layers become positively charged due to ion exchange. As a result, the positive charge is balanced because of intercalating of exchangeable anions and Charge compensating between different layers [56, 57]. One of main characteristics of LDH materials is their complex chemical composition. An enormous variety of divalent cations, including Mg^{2+}, Ni^{2+}, Zn^{2+}, Cu^{2+}, Mn^{2+}, Fe^{2+}, Co^{2+}, Ca^{2+}, etc., and trivalent cations, such as Al^{3+}, Fe^{3+}, Cr^{3+}, Mn^{3+}, Ga^{3+}, Co^{3+}, V^{3+}, etc. can be freely combined as a constituent of the versatile chemical composition of LDH. Apart from these common divalent and trivalent cations, LDH structures with monovalent (such as Li^{+}) [58], is also claimed as one of alternative materials to form LDH chemical composition. In addition, rare-earth cations [59] and various tetravalent cations (i.e. Zr^{4+} [60], Sn^{4+} [61] and Ti^{4+} [62]) have been claimed as the LDH composition materials at the same time. However, it is still controversial to prove the existence of these cations in the brucite-like layer [63]. It is claimed that the continuous LDH layers are connected together by means of weak hydrogen bonds, which is provided by molecular water with the surrounded intercalated anions. The properties of interlayer anions are very diverse. Common interlayer cations including organic and inorganic anions, such as CO_3^{2-}, NO^{3-}, SO_4^{2-}, halides, etc. [64]. Numerous other negatively charges types, for instance, anionic drugs, biomolecules [65], polyoxometalates [66], coordination compounds [67, 68], polymers [69] have also been proven to possess intercalating ability.

2.2.2 Properties

LDH materials have numerous of characteristics and functions[70], the first of which is that LDH materials is alkaline. For instance, the Mg-Al-LDH laminate consists of a magnesium octahedron and an aluminum-oxygen octahedron, in which the Al atom and the hydroxyl group are respectively located at the center and the top of the regular tetrahedron, so that the LDH are strongly alkaline. Secondly, interlayer anions in LDH structure are exchangeable[71, 72]. The exchangeability of interlayer anions in LDH is one of the most representative important properties of LDH. For the inorganic anions in the LDH material of the inorganic anion intercalation, the lower the valence state, the easier it is to be exchanged between the layers. However, according to previous researches[73], the exchange order of inorganic anions outside the LDH layer is: CO_3^{2-} > SO_4^{2-} > HPO_4^{2-} > F^- > Cl^- > $B(OH)^{4-}$ >NO^{3-}. In addition, "memory effect" is also recognized as one of typical characteristics of LDH. This means that LDH form a composite metal oxide LDO after calcination at a certain temperature. Adding it to an anion solution for reaction, LDH can partially restore the ordered layered structure[80, 81]. LDH also has thermal stability. When heated to a certain temperature, LDH will decompose. The thermal decomposition process involves the steps of first delaminating the inter-water, then de-carbonate ions and dehydrating the hydroxy groups of the laminate. When the temperature in the air is lower than 200 °C, heating the LDH only loses interlayer water and has no effect on its structure. However, when heated to 250-450 °C, heating the LDH will cause it to lose more interlayer water, while CO_2 is formed. When heated to 450~500 °C, CO_3^{2-} in the structure of LDH disappears and completely transforms into CO_2, forming a layered double oxide [74].

Since the chemical composition of LDH is not stable, the metal element type and ratio of the main layer of LDH, the type and number of interlayer anions, as well as structure of the two-dimensional pore can be adjusted as needed. The composition and structural variability of LDH can be modulated by the following aspects:

1) Cation in different valence. If the radius of the divalent metal cation and the trivalent metal cation in the LDH is close to that of Mg2+, the metal cation can covalently bond with the hydroxyl group. Therefore, matching regulation can be performed based on divalent and trivalent metal cations of different ionic radius in the LDH.

2) The type of interlayer anion or the amount of charge it carries. The types of interlayer anions include inorganic anions and organic anions.

3) Based on the structure equation mentioned in 1.2.2., molar ratio (x) of two different valence cations in the laminate can also influence the structure of LDH. The parameter x is generally between 0.1 and 0.5, but plenty of studies have shown that a single LDH crystal can be obtained only in a narrow range of x values (0.2 to 0.34), and no other impurity phase is formed in this specific range.

4) The content of water between layers.

5) Crystalline morphology and particle size of LDH. It is believed that the adsorption efficiency of LDH can be influenced because the specific surface area of material changes with the different morphology and particle size[75, 76].

2.2.3 Preparations

Based on the crystallization theory and colloidal chemistry theory, the nucleation rate can be controlled by adjusting the temperature and concentration of crystal nucleation. At the same time, the growth rate of the crystal can be controlled by influencing the crystallization time, concentration and environmental temperature. Therefore, the directional control of the crystal structure and size of the LDH can be achieved by controlling these influencing variables. The preparation methods of LDH are generally recognized as coprecipitation method, ion exchange method, hydrothermal synthesis method, calcination recovery method, urea decomposition method, and microwave crystallization method. In this part of thesis, methodologies including coprecipitation and hydrothermal synthesis are introduced:

a) Coprecipitation

The coprecipitation method is further divided into the coprecipitation condition in a low saturation coprecipitation and a high supersaturation coprecipitation. Based on previous researches, the synthesis process of the low-saturation coprecipitation method is as follows: firstly, the metal salt solution is formulated into a mixed salt solution A of a certain concentration with a certain ratio. Then, according to the specific requirements of the experiment, the NaOH and Na_2CO_3 were mixed into an alkali solution B in a certain ratio. Formerly, the mixed solution A and the mixed alkali solution B were simultaneously dropped into a beaker at a certain dropping rate and vigorously stirred. In this reaction system, the pH value was maintained constant. After consummation of titration, the solution is kept stirring and

the aging effect is carries out. Finally, the product is obtained after filtration, washing and drying. As to the synthesis process of high-saturation coprecipitation method, to begin with, the mixed salt solution and the mixed alkali solution are respectively preheated to the temperature that required for the reaction. Secondly, the secondary distilled water is added into a beaker and heated to the same temperature as the mixed solution at the same time. Then, the two solutions are simultaneously poured into the large beaker containing the secondary distilled water previously heated and keep vigorous stirring. The target LDH products is finally obtained through this process. Based on previous researches, Yang et al. prepared Mg–Al and Zn–Al LDH materials co-precipitation method at a constant pH of 9–10, which showed a splendid removal ratio of phosphate onto Zn–Al LDH and Mg–Al LDH, respectively reaching 95%. [77-79].

b) Hydrothermal synthesis

Same as coprecipitation method, in order to produce target LDH materials, mixed salt solution and the mixed alkali solution are also firstly required to be compounded. After, the salt solution and the alkali solution are slowly added together and then mixed by rapid stirring. Then, then the obtained slurry is quickly transferred to an autoclave and aged for a certain temperature (usually 100 °C) for a certain period. Finally, the product is obtained by filtration, washing, drying and grinding. One of the characteristics of this method is the separation of the nucleation and crystallization process of LDH. At the same time, the crystallization process can be promoted by increasing the aging temperature and pressure[80, 81].

2.2.4 Modifications

At the structural level, LDH have nanoscale interlevel voids, the

exchangeability of interlayer anions, and the diversity of targets that can be exchanged. These properties give LDH numerous excellent properties. At present, the interlayer modification of LDH is mainly achieved by the anion exchange modification and polymer embedded modification.

a) Anion exchange

As the host material, the ion between the LDH layers can be exchanged either by inorganic anions or organic anions. Based on current researches, the most used inorganic anion present is polyoxometalate anions[82]. However, since LDH have a high charge density, which is greater than or equal to 0.04e/A°, and it does not swell in water environment, there are potential problems during the ion exchange reaction.

b) Embedded polymer

In recent years, it has been paid increasing attention to develop the formation of organic/inorganic hybrids by high molecular weight embedded in layered inorganic materials, which is a hot field in the research of nanocomposites. The inorganic host material for embedding includes silicate clays, phosphates, metal oxides, etc. The interlayer spacing is generally between a few angstroms and tens of angstroms, and the interlayer spaces tend to have activity and can serve as a host site for chemical reaction with certain organic molecules. Because of the layered structure, LDH can be used as a host material for embedding organic molecules. Recently, the development of applying organic polymer embedded LDH to prepare novel nanocomposites has attracted great attention by worldwide researchers[83]. Rojas et al. tried to modify LDH materials with EDTA, in order to remediate heavy metals pollution. By means of an exchange method, the polydentate ligand was introduced in a

Zn-Al-LDH. The elimination process applying this LDH materials reached equilibrium in less than 30 minutes and the metal cation concentration in the wastewater was below 0.05 PPM [84].

2.3 LDH materials applications

2.3.1 Recent studies

Because of the anionic-exchange ability of LDH with organic/inorganic anions, modified LDH materials are considered as expectational materials for wastewater treatment. Table 2 reviews the adsorption capacity of Cr ions on recently reported modified LDH materials. Compared to traditional LDH alone, modified LDH materials show greater adsorption ability of pollutants because of their advantages in higher anion exchange tendency [85,86], better stability [87], larger surface area [88,89] and excellent selectivity for different metal ions [90,91]. Due to these excellent characteristics, LDH materials are capable adsorbents in water treatment applications. Based on the literature, the mainly used modified LDH materials wastewater treatment are synthesized by different techniques such as coupling of LDH with EDTA [92], and with some other compounds like MnO_2 [93], Fe_3O_4 [94], nano zero valent iron [95]) and polymers [96].

It is also observed from Table 2 that the pH conditions of all the listed LDH materials to remove Cr in wastewater are acidic (the smallest is 2 and the largest is 6), and the temperature of the experimental environment is controlled at low temperature (minimum 25 degrees, maximum 50 degrees). It can be speculated that different environmental conditions affect the efficiency of Cr removal from wastewater by LDH materials, so the influencing factors on Cr removal should be deeply discussed.

2.3.2 Influencing factors

In the literature, factors influencing the efficiency of removal heavy metal ions from wastewater by LDH materials are grouped into four categories: coexisting anions in solution, pH value, experimental temperature and the initial concentration of heavy metal ions in wastewater. Therefore, in the subsequent experiments of this study, these four factors need to be controlled in order to obtain better and stable removal effect of Cr^{6+}.

a) Coexisting anions

Grover[97] found that based on bauxite LDH materials, the effect of the influence of divalent and monovalent anions on the removal of As(VI) was ordered as: CO_3^{2-} > SO_4^{2-} , Cl-> NO_3^-. At the same time, it was also reported that the negative effect of divalent anions on the removal of As(VI) is higher than that of monovalent anions.

Pshinko [98] prepared Zn/Al-LDH by electrophoretic deposition. At the same time, EDTA, DTPA and HMDTA were utilized to form modified LDH materials, the resources of which were based on Zn/Al-LDH materials. The results show that the adsorbent material can also be applied to the purification of uranium-containing water under the conditions of increased concentration of CO_3^{2-} and HCO_3^- in natural water. In addition, it was confirmed that the Zn/Al-EDTA-LDH adsorbent can maintain high adsorption efficiency for U(VI) even in a high CO_3^{2-}concentration environment. This is very important for the uranium treatment plant to treat wastewater

Table 2. Summaries of adsorption of Cr on different LDH materials

Modified LDH materials	Surface area (m^2/g)	Pollutants	Adsorption conditions			Adsorption capacity (mg/g)	Isotherms/kinetics	Regeneration	References
			pH	Temp (℃)	Time (h)				
$CaFe_2O_4$/poly o-phenylenediamine/MgAl		Pb			0.08	1000	Langmuir/2nd order		[99]
		Cr			0.08	500			
Cl/MgAl		Cu	4-6	30	2	143.85			[100]
		Cr	4-6	30	0.5	112.7			
Calcined Graphene/MgAl	34.97	Cr	2	20	24	172.55	Freundlich/2nd order	0.1 mol/L (NaOH and Na_2CO_3) for 12 h (3 cycles)	[101]
Fe^{2+}/MgAl		Cr		30	24	649.87	Langmuir/2nd order		[102]
Fe_3O_4/C/MgAl		Cr	6	40	1	152	Langmuir/2nd order	1 mol/L NaOH (6 cycles)	[94]
MnO_2/Fe_3O_4/GO	60.1	Cr	5	40	2	175.4	Langmuir/2nd order	Alkaline solution (5 cycles)	[103]
Egg shell/MgAl membrane		Cr	5.1	25	0.5	27.9	Langmuir/-		[104]
Vermiculite/MgAl		Cr	6	30	24		Langmuir/2nd order	0.01 mol/L Na_2CO_3 (10 cycles)	[105]

Table 2 (continued)

Modified LDH materials	Surface area (m^2/g)	Pollutants	Adsorption conditions			Adsorption capacity (mg/g)	Isotherms/kinetics	Regeneration	References
			pH	Temp (℃)	Time (h)				
EDTA/NiFe2O4/ZnAl	1.5	Cr	6	25	2	64.28	Langmiur/2nd order		[106]
Carbon/MgAlO	285	Cr	5.5	50	2	172.94	Langmiur/2nd order		[107]
Nano zero valent iron/MgAl	42.2	Cr							[95]
Ni/MgAl	179	Cr		30	0.9-2.2	103.4	Langmiur/2nd order		[108]
		Congo red	7			1250			

containing high concentrations of carbonate and bicarbonate.

In summary, when applying gibbsite LDH material to remove heavy metals, the interference effects of divalent and monovalent anions is ordered as: CO_3^{2-}>SO_4^{2-}, Cl^->NO^{3-}. And compared to the monovalent anion, the negative effect of divalent anions on the removal of heavy metals is higher. Therefore, when applying LDH to remove heavy metal ions from wastewater, the interference of coexisting anions should be taken into consideration and avoided, in order to prevent it from affecting the removal of heavy metal ions.

b) pH value

The LDH material itself is alkaline, and pH has a great influence on the LDH material in the solution. At lower pH value, the LDH is easily dissolved to cause structural changes; on the other hand, in different pH conditions, different heavy metal ions exist in different ion forms. Therefore, pH has a great influence on the adsorption of heavy metals by LDH materials.

Gong et al.[109] prepared LDH-NCs@CNs Nano-assembly materials by assembling LDH nanocrystals (LDH-NCs) onto the surface of nano-carbon spheres (CNs) and applying them to the treatment of heavy metals from wastewater, and the effect of different initial pH on the adsorption of Cu^{2+} was studied. When the pH value was between 2 and 6, the adsorption amount of the material increased with the increase of pH, while when the pH value is greater than 6, the amount of adsorption decreases as the value of p H increases. Meanwhile, when the initial pH value is less than 4, the amount of Cu^{2+} adsorbed by the material is small because the LDH-NCs@CNs nano-assembly material is partially dissolved due to its acidic hydrolysis property. When the pH value is 4.0 to 7.0, the removal rate of

Cu2+ is over 94%, which indicates that the LDH-NCs@CNs nano-assembly material can maintain good adsorption performance in the natural environment without additionally adjusting the initial pH value. And when the pH value is greater than 8.0, the adsorption capacity of the material is greatly reduced, which may due to that Cu^{2+} is hydrolyzed and polymerized when the pH value is greater than 7. Heavy metal ions are able to form a variety of polymers in water. For example, when p H > 7, Cu2+ will be hydrolyzed to form $Cu(OH)^{+}$, $Cu(OH)_2$ and $Cu(OH)_3^{-}$. Hydrolysis and polymerization of heavy metal ions directly reduce the adsorption capacity of LDH-NCs@CNs nano-assembly materials.

The results mean that the optimal pH value for removal of heavy metal ions by LDH from water is 6. When the pH value is between 2 and 6, the LDH material dissolves due to the acidic nature of the solution, so the removal effect increases as the pH value increases. When the pH value is between 6 and 8, the LDH material removal effect decreases as the pH value increases due to hydrolysis and polymerization of heavy metal ions. Therefore, considering the use of LDH materials to remove heavy metal ions, maintaining the solution pH value of 6 can improve the removal of heavy metal ions by LDH.

c) Temperature

Temperature may have two main effects on the adsorption process. The diffusion rate of the adsorbent molecules in the outer boundary layer and pores increases with the rise of temperature. In addition, changing the temperature influences the equilibrium adsorption capacity of the specific adsorbent. Zhang et al.[110] synthesized Fe_3O_4/C/Mg Al LDH nanomaterials to remove hexavalent chromium ions from water. The study found that the material can efficiently adsorb and remove hexavalent chromium ions in

water, and the temperature influences the adsorption effect. The results showed that when the temperature is increased from 15 °C to 40 °C, the equilibrium adsorption capacity of the material for Cr (VI) increases from 120.5 mg/g to 152.0 mg/g with temperature, and reached the maximum equilibrium adsorption capacity at 40 °C. When the temperature was higher than 40 °C, the equilibrium adsorption capacity of the material for Cr (VI) was rapidly reduced and was reduced to 129.3 mg/g at a temperature of 60 °C.

Summarily speaking, the most suitable temperature for the removal of heavy metal ions by LDH materials should be 40 °C. When the temperature is below 40 °C, the amount of heavy metal removal increases with cumulative temperature, while in the temperature range of more than 40 °C, the amount of removal decreases with increasing temperature. Therefore, considering the use of the LDH material to remove heavy metal ions, maintaining the solution temperature at 40 ° C can improve the removal of heavy metal ions.

d) Initial concentration of heavy metal ions

The initial concentration of heavy metal ions affects the adsorption process mainly because the high concentration targets heavy metal ions provide a higher driving force to promote the target heavy metal ions into the LDH materials. Therefore, it can be inferred that the removal efficiency increases as the concentration of heavy metals in the solution enlarges.

Chen et al[111] used the co-precipitation method to prepare Ca/Al-DS LDH by applying sodium dodecyl sulfate (SDS) modified calcium aluminum LDH as basic materials, and studied the removal mechanism of heavy metal

cations Ni^{2+}. It was found that the maximum removal amount of Ni^{2+} was 143.79 g/g, and the removal mechanism was mainly recognized as surface complexation, isomorphous substitution and adsorption of $CaCO_3$. At the same time, it was also studied that columnar inter-layer organic anions may help to maintain the layered structure of the LDH. This research revealed the mechanism of multivariate interaction between heavy metal ions and Ca/Al LDH. Additionally, a method was proposed for generating novel LDH with organic interlayers, which is achieved by isomorphic substitution. The effects of initial concentration of different Ni^{2+} on 0 to 8.5mmol/L (0-500mg/L) on the adsorption process and effect were also studied. It was found that when the initial concentration of Ni^{2+} was less than 1mmol/L, the removal of Ni^{2+} was 99.73 mg/g, and when the initial concentration of Ni^{2+} is 1.0 to 1.4mmol/L, the adsorption amount decreases from 99.73mg/g to 82.17mg/g. Then, as the initial concentration of Ni^{2+} increases, the removal amount maintains a linear increase from 82.17 mg/g to 146.73 mg/g. Under alkaline conditions, Al^{3+} on Ca/Al-DS LDH is released as $Al(OH)^{4-}$. When the initial concentration of Ni^{2+} is low, the Ca^{2+} released by Ca/Al-DS LDH gradually increases, while the release of $Al(OH)^{4-}$ in the solution decreases with the increase of the initial concentration of Ni^{2+}. Meanwhile, when the initial Ni^{2+} concentration in the solution raised from 0.0 mm/L to 1.0 mmol/L, the release of Ca^{2+} improved from 1.1 to 1.2 mmol/g, while the release of $Al(OH)^{4-}$ reduced from 0.7 to 0.0 mmol/g. Subsequently, the amount of released Ca^{2+} decreased to 0.07 mmol/g, and as the initial Ni2+ concentration continued to increase, the release amount of $Al(OH)^{4-}$ was always maintained at 0.0 mmol/g. This indicated that Ca^{2+} and $Al(OH)^{4-}$ on Ca/Al-DS LDH were also involved in the reaction and influenced the removal of Ni^{2+}.

In summary, the removal efficiency of heavy metal ions by LDH improved with the increase of concentration of the heavy metal ions to be removed.

Therefore, in consideration of the use of the LDH material to remove heavy metal ions, the removal effect of heavy metal ions can be improved by increasing the concentration of heavy metal ions to be removed without additionally increasing the cost.

Chapter 3 Experimental

3.1 Methodology

In this study, A fixed ratio (Mn:Al=2:1) Mn/Al-LDH material was prepared by hydrothermal synthesis and characterized by XRD, SEM, BET, TEM, and XPS. XRD analysis was carried out to see whether the synthesized materials have the base-derived characteristic peaks of typical LDH materials. Based on this, it was judged whether the LDH materials were successfully synthesized. The morphology of the material particles was observed by SEM to determine whether it was a layered structure of typical LDH materials. The specific surface area of the composite material was obtained by BET characterization to compare the adsorption properties of the two materials. The TEM was used to observe whether the material is a regular hexagonal crystal structure of typical LDH. Finally, the valence state and bonding state of the metal ions on the LDH material can be known by XPS characterization, thereby judging whether the synthesized material is a Mn^{2+} type LDH material. For the purpose of testing the application possibility of prepared LDH materials in wastewater, the prepared LDH material was applied to remove Cr^{6+} from water, and the effect of pH on the removal effect was investigated. In order to study the effects of the application of the material in the natural environment, a quantitative Cr^{6+}-containing solution was prepared with $K_2Cr_2O_7$. Formerly, NaOH solution was added to adjust different initial pH, and then a quantitative amount of Mn/Al-LDH material was added to carry out the adsorption reaction to study the effect of different pH on the adsorption of Cr^{6+} ions on the material. The effect of general anions on the reaction should be controlled during the preparation of the $K_2Cr_2O_7$ solution. Finally, through a variety of characterization methods, the removal mechanism of the material on the pollutants is obtained. As to the modified LDH materials, in this study, based on the

previous research, the Mn/Al-LDH material was modified to synthesize Zeolite-Mn/Al-LDH, which further improved the efficiency of Ni ion removal. This study explores the removal efficiency of Ni ions in water by Zeolite-Mn/Al-LDH materials, and the change of pH value in water is monitored. The reaction mechanism was explored by XRD, SEM, TEM and XPS characterization.

3.2 Chemicals and reagents

The reagents and chemicals applied in this chapter are listed as Table 3-1.

Table 3-1 The main experimental chemicals and reagents

Chemicals	Molecular formula	Standard	Supplier
Magnesium chloride tetrahydrate	$MnCl_2 \cdot 4H_2O$	AR	Shanghai Aladdin Biochemical Technology Co., Ltd.
Aluminum chloride hexahydrate	$AlCl_3 \cdot 6H_2O$	AR	Shanghai Aladdin Biochemical Technology Co., Ltd.
Sodium chloride	NaCl	AR	Sinopharm Chemical Reagent Co., Ltd.
Sodium hydroxide	NaOH	AR	Sinopharm Chemical Reagent Co., Ltd.
Zeolite	-	-	Ningbo Wesdon Powder Pharma Coating Co., Ltd

$MnCl_2 \cdot 4H_2O$ and $AlCl_3 \cdot 6H_2O$ are both supplied by Shanghai Aladdin Biochemical Technology Co., Ltd. NaCl and NaOH are provided by Sinopharm Chemical Reagent Co., Ltd. And the supplier of zeolite is Ningbo

Wesdon Powder Pharma Coating Co., Ltd. $MnCl_2 \cdot 4H_2O$ and $AlCl_3 \cdot 6H_2O$ are the core raw materials of LDH, and their purity is over 99.8%, both of which are laboratory grade (AR). In addition, both the NaOH as the pH adjuster and the NaCl in the anion environment of the control solution also reached the AR level. The zeolite material was a solid cake which was ground to a powder for subsequent experiments and sieved through a 1 um sieve.

3.3 Preparations

3.3.1 Mn/Al-LDH

2M 50mL of $MnCl_2 \cdot 4H_2O$ and 1M of 50mL of $AlCl_3 \cdot 6H_2O$ were respectively prepared so that the molar ratio of metal ions of Mn^{2+} to Al^{3+} was 2:1. Add the weighed $AlCl_3 \cdot 6H_2O$ to a beaker containing 210 mL of DI water at room temperature, place the beaker on a magnetic stirrer, adjust the temperature to 25 ° C, rotate at 500 rpm, and seal the beaker with plastic wrap and keep stirring. The weighed $MnCl_2 \cdot 4H_2O$ was then added to the above beaker while 100 mL of 1 M NaCl solution was added to control the anion in the solution. Formerly, by continuously adding the existing 2 mol/L NaOH solution to maintain the pH of the aqueous solution at about 9, the resulting suspension was immediately transferred to a 500 mL Teflon container and kept at 80 ° C for 24 hours. After 3 times of 200 mL of deionized water solution and 2 times of 100 mL of ethanol solution, the mixture was centrifuged to obtain a solid product, which was finally dried at 40 °C. The obtained solid was ground into a powder, which was formally sealed and stored.

3.3.2 Modification

Similar as the process preparing normal Mn/Al-LDH, in order to prepare the

LDH modified by zeolite, the modified material was added during the process of chemical synthesis. To be specific, zeolite was firstly ground into powder and then screened with a sieve to control the size of the zeolite powder below 1 um. Formerly, same as previous process of preparing Mn/Al-LDH, firstly, 2M 50mL of $MnCl_2 \cdot 4H_2O$ and 1M of 50mL of $AlCl_3 \cdot 6H_2O$ were respectively prepared. Next, ground zeolite powder was mixed with weighed $AlCl_3 \cdot 6H_2O$, and then weighed $MnCl_2 \cdot 4H_2O$ was added to the above beaker while 100 mL of 1 M NaCl solution was added to the above beaker and 100 mL of 1 M NaCl solution, at the same time, was added to control the anion in the solution. Then, the pH of the aqueous solution was maintained at about 9 by continuously adding the existing 2 mol/L NaOH solution. The remaining process including hydrothermal reaction, purification, drying was same as preparing normal Mn/Al-LDH. Finally, the Zeolite-Mn/Al-LDH powder was obtained. In order to recognize the physical properties of the prepared material from a microscopic level, a series of characterization steps were applied.

When the preparation of Mn/Al-LDH and Zeolite-Mn/Al-LDH is complete, characterization including XRD, SEM, TEM and BET was applied to firstly determine the chemical composition of the material, and then recognize the chemical structure and morphology of these two LDH materials.

The two materials have been characterized by XRD, SEM, TEM and BET before the adsorption reaction. It is found that the prepared LDH have the basic crystal layer structure and physical adsorption properties of typical LDH materials. On this basis, the prepared Mn/Al-LDH and Zeolite-Mn/Al-LDH materials were applied in this study to the removal of hexavalent chromium ions in water, and the efficiency of Mn/Al-LDH and Zeolite-Mn/Al-LDH removal of hexavalent chromium ions was compared. The LDH material with better removal effect was further explored.

The main laboratory equipment used in this chapter is shown in Table 3-3:

Table 3-3 The main experimental instruments

Equipment	Type
Analytical Balances	EN1862
Thermostatic oscillator	ZTH-82
Magnetic stirrer	85-1

Firstly, a $K_2Cr_2O_7$ solution having a concentration of 1 mmol/L was prepared, and 15 ml of which was placed in nine centrifuge tubes, No. 1-No. 11. Among them, the No.1-No.5 tubes were used to test the adsorption ability of Zeolite-Mn/Al-LDH at different length of adsorption times (5min, 15min, 30min, 60min, 90min, respectively) and No.5-No.8 tubes were applied for testing the adsorption ability of traditional Mn/Al-LDH in different period of time (same as No.1-No.5). And the No.11 tube with 15mL 1 mmol/L $K_2Cr_2O_7$ solution was identified as a control group without any adsorbents. Put all tubes into a constant temperature oscillator, set the temperature to 25 ° C, rotate at 150 rpm, and take the corresponding solution tubes from the oscillator at 5, 15, 30, 60 and 90 minutes. The pH was firstly measured, and then about 15 mL of the solution was filtered with a filter syringe, and the filtrate was stored for the testing of Cr^{6+} ion concentration and total chromium concentration in the solution. The remaining solution was taken for suction filtration, and after the water in the solution was drained, a tube of ethanol was added to continue a second filtration. After the end of the suction filtration, the obtained solid was taken out together with the suction filter paper and placed on the folded weighing paper, and placed in a vacuum drying oven at a temperature of 50 °C. After the solid is dried, it is taken out and left for characterization.

3.4 Characterization overview(XRD, SEM, TEM, BET)

3.4.1 Morphology and Surface Elements Analysis (SEM, TEM)

Scanning electron microscope (SEM) is a category of electron microscope that produces images achieving resolution better than 1 nanometer of samples by emitting a focus beam of electrons to the surface. Compared to SEM, not only does transmission electron microscopy (TEM) have a higher magnification, but the dispersion of nanoparticles in the polymer can also be observed.

Firstly, Small pieces (around 1 cm ×1 cm) were cut off from each LDH sample and attached to the stages with conductive adhesive. since the LDH were not conductive, it is required to spray gold coating with gold spray machine. As to the instrument setting information, the SEM type applied in this study is SEM-EDS (ZEISS, EVO 18; Oxford Company), which was used for analyzing morphological characterization and element composition of LDH materials. The main composition of SEM-EDS consists of the following parts: electron beam, collimator, electron trap and semiconductor crystal detector. The SEM-EDS mode is adjusted to SE 2. The instrument parameters are as follows: energy 8 kV (acceleration voltage 0.5-30 kV) and accuracy, 10% of detection limit, 500,000. The TEM images were obtained on a Hitachi H-800 transmission electron microanalyzer. The accelerated voltage in this study is set to 200 kV and the camera length was 0.8 m.

3.4.2 Material composition (XRD)

X-ray diffraction (XRD) is an instrument to analyze the atomic and molecular structure of a crystal sample. By measuring the angle and intensity of these diffracted beams, a three-dimensional image of the

electron density in the crystal can be created. Due to complicated composition LDH materials and the modified production, it is more reliable to co-analyze the mineral composition of LDH by SEM-EDS and XRD, in order to verify the metal and mineral composition in LDH. Since diffraction effects are largely affected by sample preparation, it is required to make sure that the particle size is sufficient for analysis. First, filters were cut into small pieces and place in the sample slot. Next, slightly press each piece with wool glass so that the flat surface of each sample is flush with the slot surface. The XRD applied in this study is the D8 Advance produced by the German Bruker-AXS company. XRD is mainly composed by a detector, X-ray source and adjustment system. The scanning mode in this study is set to 2Theta/Theta mode and the parameters setting are as followed: scanning speed, 1° (2 θ)/min; scanning range, 5~80°; Incident slit 1/2°; CuK α radiation (λ=1.54056° A); X-Ray information: 40kV/30mA.

3.4.3 Specific surface area (BET)

The porosity and surface area of LDH samples were tested by BET surface area analysis (Micromeritics Tristar II 3020). BET and Langmuir surface area, BJH pore volume, distribution and porosity data were observed from provided results. Samples were weighed to around 0.13 g and the analysis bath temperature was set to -195.85°C. The degas process lasted for 8 hours. Equilibration interval was set to 10s and sample density is 1.00 g/cm³.

Chapter 4 Removal of Cr^{6+} by LDH

In this chapter, XRD, SEM, TEM, and BET characterization results are shown and analyzed. The results of XRD show that Mn/Al-LDH and Zeolite-Mn/Al-LDH have typical LDH-like layered structure. Through TEM, it was found that both Mn/Al-LDH and Zeolite-Mn/Al-LDH possess a regular hexagonal crystal structure. The SEM results indicate that the modified Zeolite-Mn/Al-LDH have a porous structure which is not found in ordinary Mn/Al-LDH. Such a structure can make Zeolite-Mn/Al-LDH have a larger specific surface area and better adsorption capacity, which was also confirmed in BET characterization result. After adsorption test, it was known that Zeolite-Mn/Al-LDH reaches the critical point of adsorption earlier than Mn/Al-LDH.

4.1 Characterizations results

4.1.1 XRD

X-ray diffraction (XRD) identifies the phase and composition of a sample based on the position and intensity of the characteristic peak. In this experiment, the sample was characterized by a D8 Advance X-ray diffractometer from Bruker, Germany, and the working conditions were: Cu target, step size 0.08. The Mn/Al-LDH and Zeolite-Mn/Al-LDH raw materials were characterized by XRD, and the results are shown in Figure 4-1.

(a)

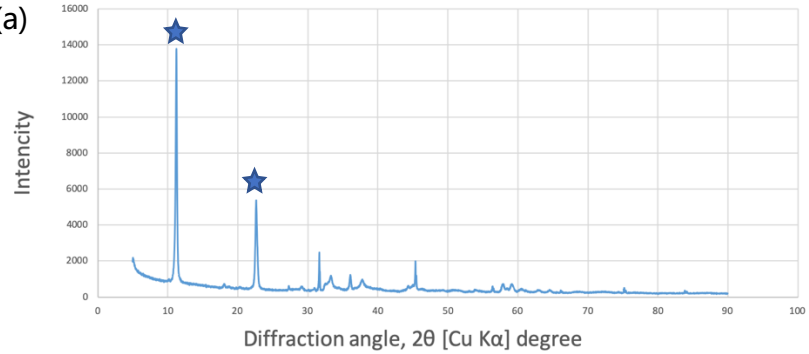

(b)

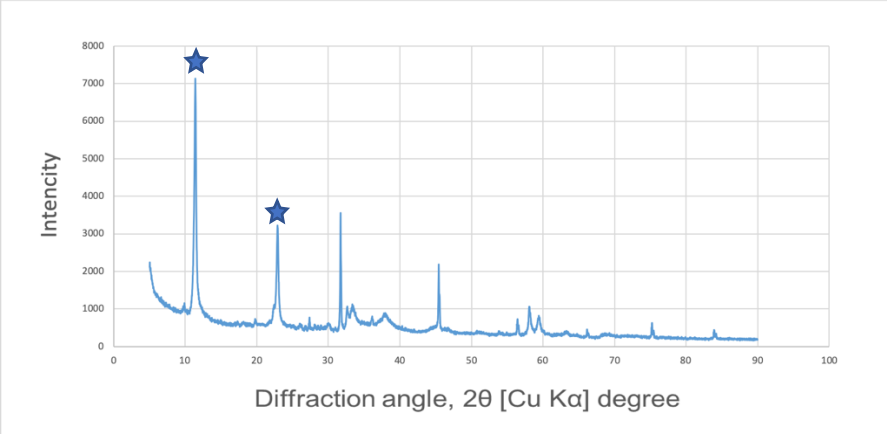

Fig. 4-1. XRD patterns of Mn/Al-LDH (a) and Zeolite-Mn/Al-LDH (b) before adsorption. ☆: the characteristic diffraction peaks of the 003 (11.5°) and 006 (23.2°) crystal planes.

The LDH material was characterized by XRD before the adsorption reaction. Based on the figure, the basic characteristics of the diffraction peaks in the spectrum indicate that both Mn/Al-LDH and Zeolite-Mn/Al-LDH form a crystalline layered structure[112-114]. The characteristic diffraction peaks at 11.5° and 23.2° are observed on the XRD patterns of Mn/Al-LDH and Zeolite-Mn/Al-LDH, respectively. After comparing the diffraction peaks of these two features with the standard spectra, it is found that these two characteristic diffraction peaks respectively correspond to the characteristic diffraction peaks of the 003 and 006 crystals planes, while the characteristic diffraction peaks of the 003 and 006 crystal planes are typical characteristics of the LDH material. The thickness of the LDH interlayer region is determined by the d value (layer spacing) and the thickness of the laminate. The thickness of the laminate for general LDH is 4.8 Å[115]. The XRD characterization of Mn/Al-LDH and Zeolite-Mn/Al-LDH shows that the two LDH materials are well synthesized and have a crystalline layered structure. At the same time, the structure of Zeolite-Mn/Al-LDH is different from that of Mn/Al-LDH due to the modification of zeolite.

4.1.2 SEM

The sample was firstly placed in a golden spray instrument for gold plating to increase the electrical conductivity of the sample material. The sample was then placed on a glass slide for SEM testing to obtain a SEM image of the material to determine its particle size and morphology. The SEM characterization results of the Mn/Al-LDH and Zeolite-Mn/Al-LDH materials before the adsorption reaction is shown in Figure 5-1 and Figure 5-2, respectively. As can be seen from the figures, the morphology and crystal size of Mn/Al-LDH and Zeolite-Mn/Al-LDH can be visually observed. A flake-like particle structure was observed in the samples before adsorption of the two LDH materials. It was also found that, relative to Mn/Al-LDH, Zeolite-Mn/Al-LDH not only has a porous structure, the surface crystal particles of Zeolite-Mn/Al-LDH also aggregated to form a denser structure due to modification by zeolite. The results of this observation are mainly attributed to the dispersion of sample preparation during SEM characterization.

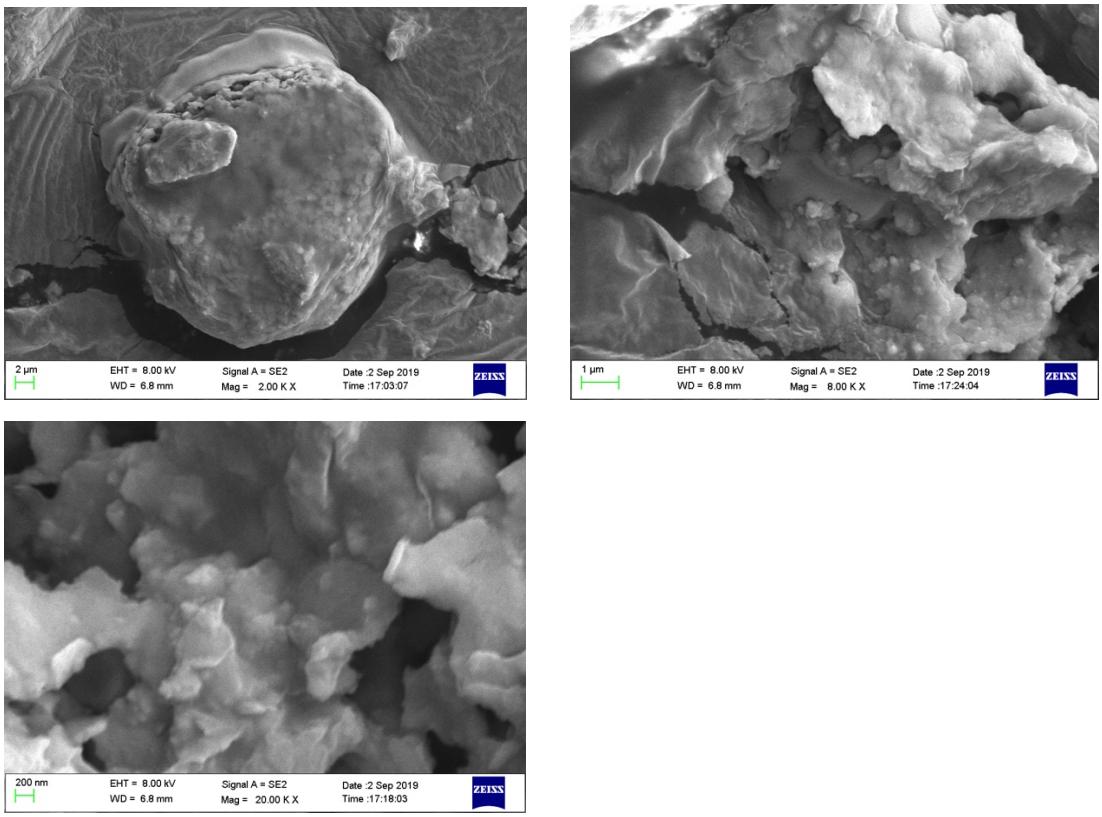

Fig. 4-2. SEM images of Mn/Al-LDH

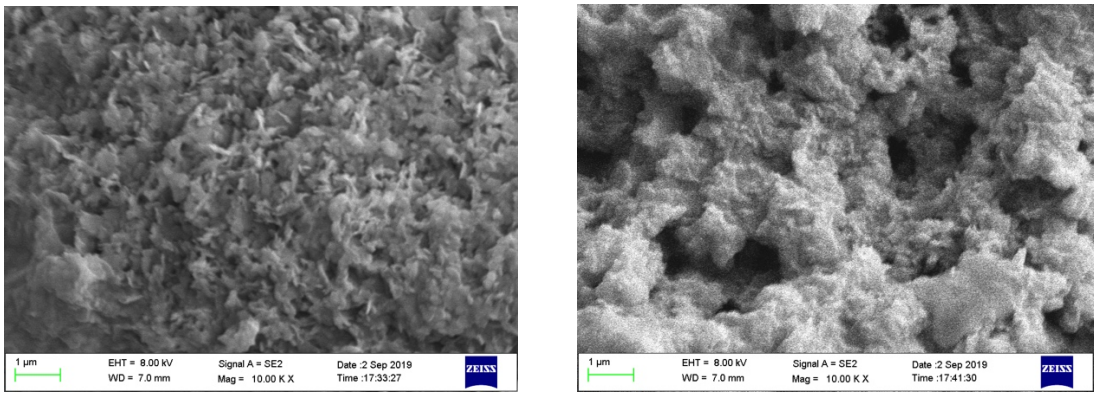

Fig. 4-3. SEM images of Zeolite-Mn/Al-LDH

4.1.3 TEM

In this study, Transmission electron microscope (TEM) was applied to detect the crystal structure and morphology of the sample material. Compared to SEM, not only does TEM have a higher magnification, but the dispersion of nanoparticles in the polymer can also be observed.

Fig. 5-3 and 5-4 shows the TEM characterization result of Mn/Al-LDH and Zeolite-Mn/Al-LDH before adsorption. As can be seen from the figure, both Mn/Al-LDH and Zeolite-Mn/Al-LDH exhibit a regular hexagonal crystal structure, which is a typical crystal shape of LDH materials. The individual particle sizes of Mn/Al-LDH and Zeolite-Mn/Al-LDH are 300 nm wide, 50 nm thick, and 200 nm wide and 35 nm thick, respectively. Moreover, Figures 2-4(c), (d) and Figures 2-5(c), (d) are high-resolution TEM representations of Mn/Al-LDH and Zeolite-Mn/Al-LDH. Corresponding to the (012) crystal plane, the lattice fringes of the Zeolite-Mn/Al-LDH sample have a pitch of 0.49 nm, and Mn/Al-LDH has a similar lattice fringe pitch, which is 0.50nm, corresponding to the (012) crystal plane.

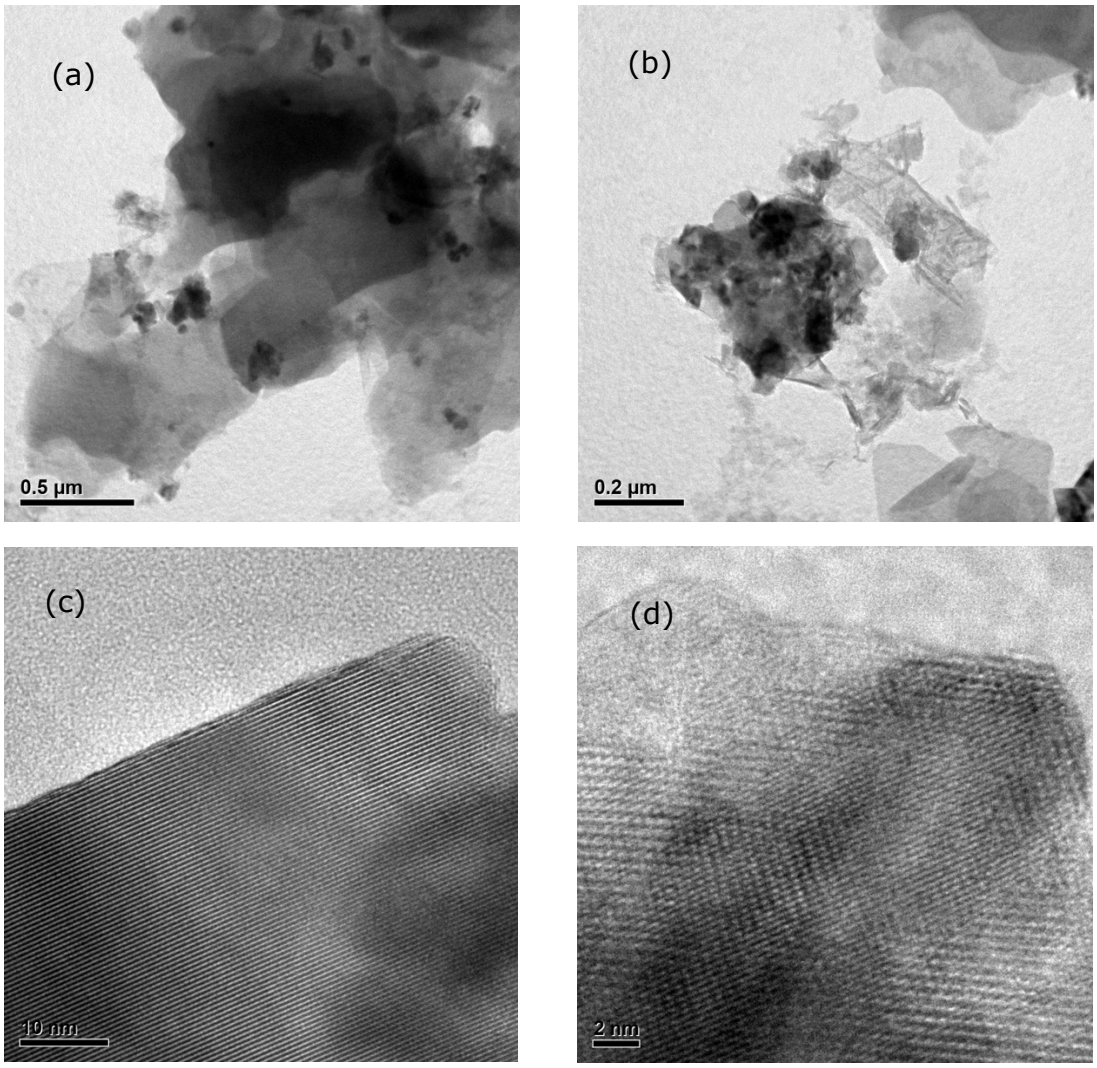

Fig. 4-4. TEM images of Mn/Al-LDH. Horizontal bars: (a): 500nm, (b): 200nm, (c): 10nm and (d): 2nm. (c) and (d) are the HRTEM images of Mn/Al-LDH, respectively.

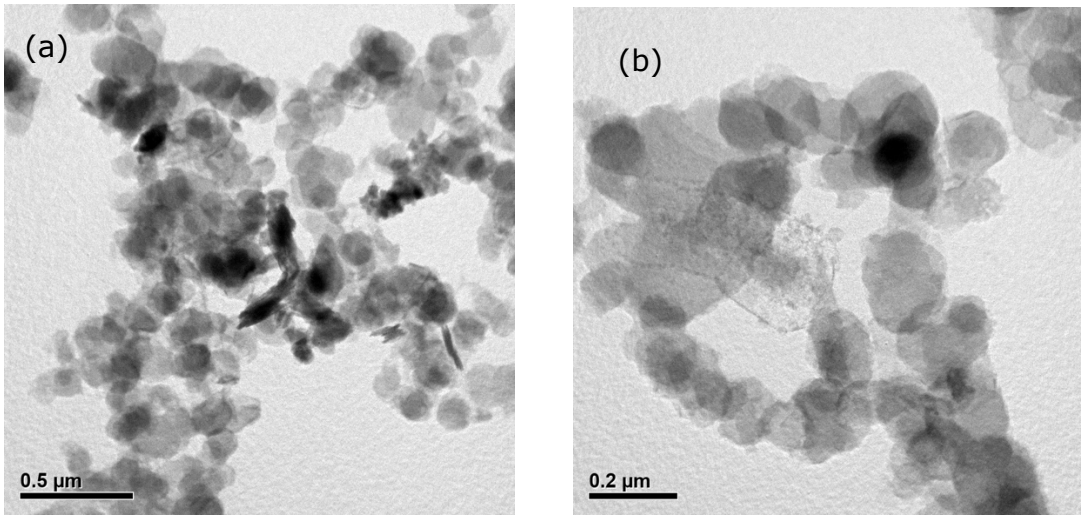

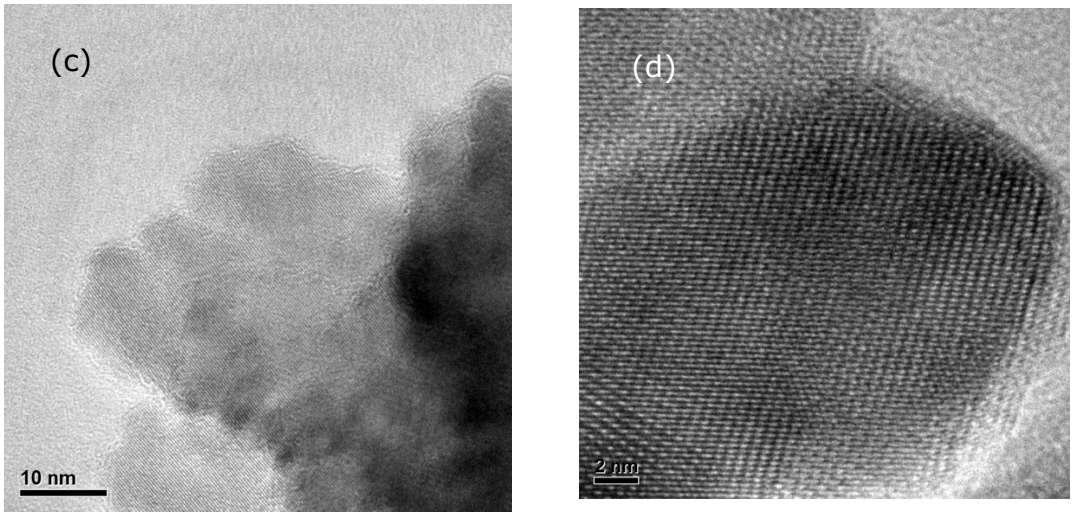

Fig. 4-5. TEM images of Zeolite-Mn/Al-LDH. Horizontal bars: (a): 500nm, (b): 200nm, (c): 10nm and (d): 2nm. (c) and (d) are the HRTEM images of Zeolite-Mn/Al-LDH, respectively.

4.1.4 BET

According to the BET characterization results, information such as specific surface area, pore volume, pore size distribution and pore type of mesoporous materials can be obtained. As to the definition of surface area, both Langmuir surface area and BET surface area can be considered as an index to describe surface area. However, even with the original data of the same sample, the calculated Langmuir surface area is significantly larger than the BET surface area. The first reason for this phenomime is that the single-layer adsorption amounts calculated by the two models are different. Langmuir adsorption model considers that only a monolayer of adsorbate can be formed on top the surface. In contrast, BET model considers multilayer formation. This means when the monolayer of adsorbent molecules completely covers the surface of the adsorbent, the adsorption amounts are different. Langmuir theory believes that the adsorption of adsorbate molecules on the surface of the adsorbent is limited to single-

layer adsorption, so the single-layer adsorption amount is the saturated adsorption amount. However, BET theory believes that the adsorption of adsorbents on the adsorption surface is not limited to a single layer, but can be multiple layers. [116]

The surface area characterization results of Zeolite-Mn-Al-LDH and Mn-Al-LDH are shown in Figure 4-6. It is known from the figure that the BET surface area values of Zeolite-Mn-Al-LDH and Mn-Al-LDH are 47.49 ± 0.11 m^2/g and 33.41 ± 0.17 m^2/g. The BJH adsorption mean pore size and pore size of Zeolite-Mn-Al-LDH are 17.7256 nm and 0.226692 cm^3/g, respectively, and the corresponding parameter values of Mn-Al-LDH are 9.3631 nm and 0.078799 cm^3/g, respectively. In addition, according to the results of surface area results, it is observed that both Langmuir surface area and BET surface area of modified Zeolite-Mn/Al-LDH are larger than normal Mn/Al-LDH. Based on the results, the Langmuir surface area of Zeolite-Mn/Al-LDH and Mn/Al-LDH is 70.5598 m^2/g and 49.7539 m^2/g, respectively. At the same time, the BET surface area of Zeolite-Mn/Al-LDH and Mn/Al-LDH is 47.4876 m^2/g and 33.4094 m^2/g, respectively. The BET characterization results indicate that the physical adsorption capacity of Zeolite-Mn/Al-LDH is greater than that of Mn/Al-LDH.

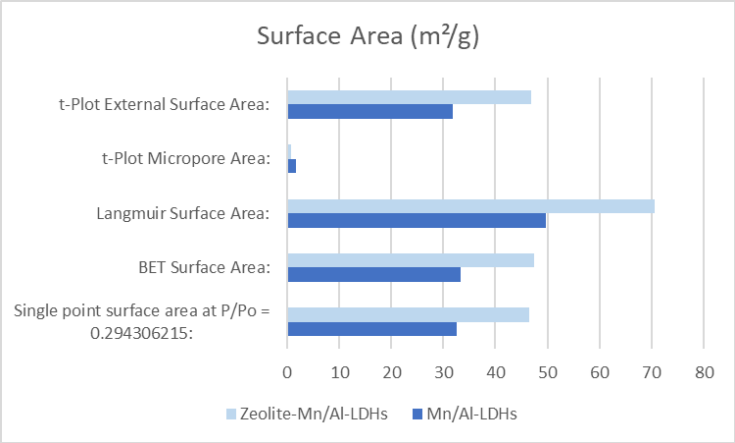

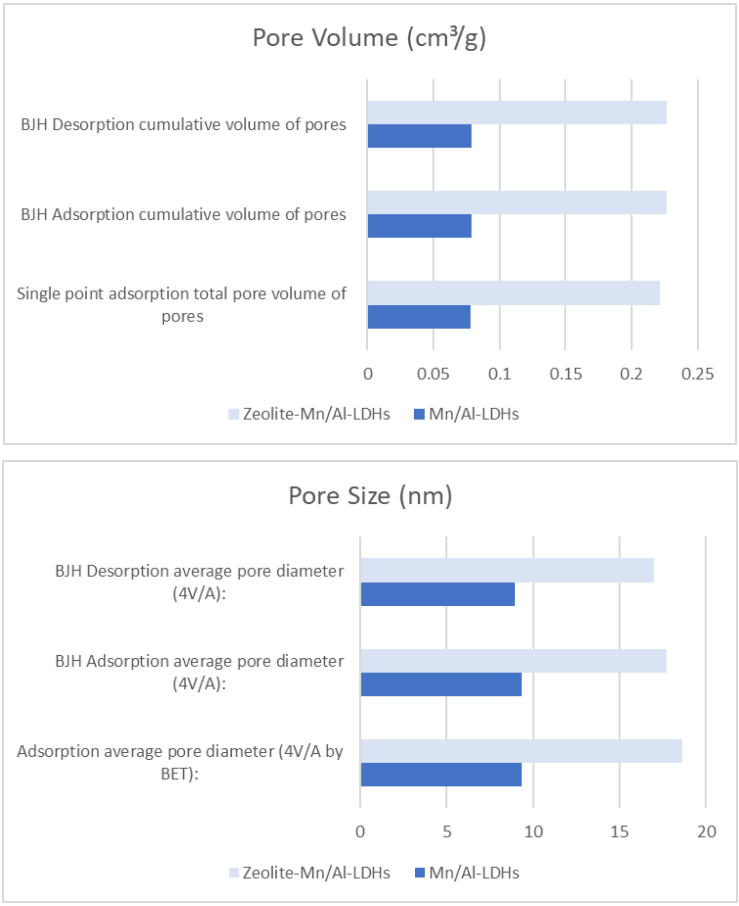

Fig. 4-6. Comparison of surface area, pore volume and pore size between Zeolite-Mn/Al LDH and Mn/Al LDH

4.2 Removal

4.2.1 Removal mechanism

Based on existing research[117], it has been proved that during adsorption of Cr^{6+} by LDH materials, Cr^{3+} and Cr^{6+} coexist on the surface of LDH materials. The appearance of Cr^{3+} proved that reduction reaction occurred during the adsorption process of Cr^{6+}. After reduction reaction, the Cr^{3+} species was attached to the surface of LDH materials. According to the research by Zhu et al., the presence of Cr^{3+} can be further confirmed by the XPS characterization. In order to further explore the adsorption mechanisms of Cr^{6+} onto LDH, it is fundamental to consider the Cr^{6+} species

in solution, as well as different types and ionic states of the functional groups present on the sorbent material. It was proved that when pH value was low, the predominant Cr^{6+} species is $HCrO_4^-$. With the increase of pH value, the predominant Cr^{6+} species is shifted to $Cr_2O_7^{2-}$. Under acidic and alkaline environment, following reactions occur as the formulas below:

$$Cr_2O_7{}^{2-} + 14H^+ + 6e^- = Cr^{3+} + 7H_2O$$

$$Cr_2O_7{}^{2-} + 7H_2O + 6e^- = 2Cr(OH)_3(aq) + 8OH^-$$

In addition, the mechanism of removing Cr^{6+} from wastewater by LDH materials has already been discussed in previous research [119]. Drawing on the results of previous studies, it is inferred that the mechanism of removing Cr^{6+} in wastewater by LDH materials in this study is the combined removal mechanism of adsorption-reduction process. When the initial pH value of the solution is 7, Cr^{6+} exists in two forms, $Cr_2O_7^{2-}$ and $HCr_2O_7^-$. Because $Cr_2O_7^{2-}$ and $HCr_2O_7^-$ are negatively charged, they will undergo ion exchange with LDH, and Cr^{6+} will be fixed into the interlayer or the surface of the Mn/Al-LDH. Once fixed, the Mn^{2+} on the LDH laminate will reduce Cr^{6+} to Cr^{3+}, and at the same time Mn^{2+} will be oxidized to Mn^{3+} and Mn^{4+}. As the number of high-valent Mn ions on the LDH laminate structure increases, the stability of LDH becomes weak. As a result, LDH releases Mn^{3+} and Mn^{4+} into the solution. The released Mn^{3+} will react with OH^- to form a $Mn(OH)_3$ precipitate, which will then be finally converted into Mn_2O_3. Besides, Mn^{4+} will be converted into a MnO_2 precipitate. During this process, co-precipitation may occur, and during the co-precipitation process different forms of Cr are fixed.

4.2.2 Removal results

Based on the literature, three main factors influencing the efficiency of removal heavy metal ions from wastewater by LDH materials are grouped into four categories: coexisting anions in solution, pH value, experimental temperature and the initial concentration of heavy metal ions in wastewater. In this study, all three influence factors were controlled in order to prevent the two LDH materials from being affected by other external factors during the adsorption process. In summary, according to the conclusion of the literature review, the pH value during the adsorption test was stabilized at 7, the ambient temperature of the experiment was controlled at 26°C, and the initial concentration of Cr^{6+} and the initial concentration of the adsorbent were fixed.

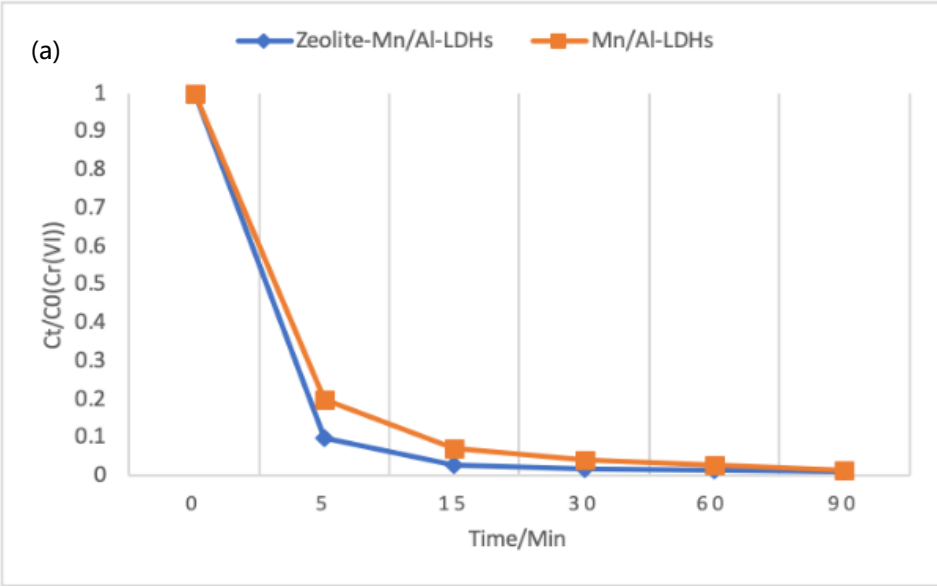

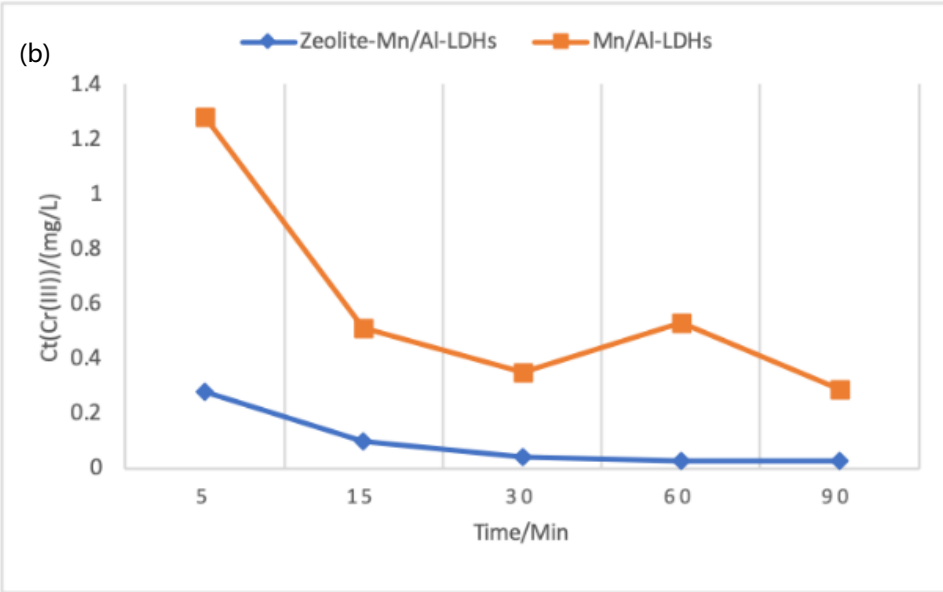

Fig. 4-7. Comparison of the adsorption efficiency of Mn/Al-LDH and Zeolite-Mn/Al-LDH to Cr(VI) (sorbent: 3.33 g/L, initial concentration of K2Cr2O7: 1 mmol/L, initial pH: 7, reaction time: 90 min): (a) detection of Cr(VI), (b) shows the concentration of Cr(III) at the same sampling time.

Figure 4-7 presents the Cr^{6+} removal efficiency of Mn/Al-LDH and Zeolite-Mn/Al-LDH. It can be seen from Fig. 4-7(a) that when the reaction time is 5 min, the removal efficiencies of Mn/Al-LDH and Zeolite-Mn/Al-LDH for Cr^{6+} ions are 78.14% and 91.38%, respectively; when the reaction time is 15 min, the removal efficiencies are respectively 89.64% and 97.7%; the removal efficiency was 95.02% and 98.19% when the reaction time was 60min, and the removal efficiency was 97.27% and 98.22% when the reaction time was 90 min. It is recognized that both Mn/Al-LDH and Zeolite-Mn/Al-LDH have the ability to efficiently remove Cr^{6+} ions in solution. However, compared to conventional Mn/Al-LDH, the modified Zeolite-Mn/Al-LDH have higher efficiency in the first 15 minutes to remove hexavalent chromium ions from water. Moreover, it can almost completely remove hexavalent chromium ions from water in a short time of 30 minutes. Therefore, Zeolite-Mn/Al-LDH has better removal ability for Cr^{6+}.

Figure 4-7(b) shows the Cr^{3+} concentration measured for the sample at the same testing time, thus also demonstrating the presence of Cr^{3+} in the solution. It can be seen from the figure that the corresponding curve of Zeolite-Mn/Al-LDH is lower than Mn/Al-LDH, and when the reaction time is 5 min, and when the reaction time is 5 min, the Cr^{3+} concentration in the solution corresponding to Mn/Al-LDH and Zeolite-Mn/Al-LDH were 1.28 and 0.28 mg/L, respectively. In addition, when the reaction time was 90 min, the Cr^{3+} concentrations were respectively 0.4 and 0.04 mg/L. It is proved that Zeolite-Mn/Al-LDH has higher adsorption capacity for Cr^{6+} and Cr^{3+} than traditional Mn/Al-LDH. The detection of Cr^{3+} from the solution explains that the possible removal mechanism of Zeolite-Mn/Al-LDH and Mn/Al-LDH for Cr^{6+} ions is a combination of adsorption and reduction. Compared with the traditional Mn/Al-LDH, the modified Zeolite-Mn/Al-LDH have a higher comparative area, which improves the adsorption capacity.

Chapter 5 Conclusions and future work

In this study, Mn-Al-LDH materials were prepared by hydrothermal synthesis and tried to modify them with zeolite. The two LDH materials were applied to the removal of Cr^{6+} in solution. By comparing the Cr^{6+} removal efficiency of Zeolite-Mn-Al-LDH and Mn-Al-LDH, the experimental results show that the modified Zeolite-Mn-Al-LDH can adsorb Cr^{6+} ion in solution faster than ordinary Mn-Al-LDH. By means of characterization, Zeolite-Mn-Al-LDH has better specific surface area than Mn-Al-LDH, which improves the adsorption efficiency of Zeolite-Mn-Al-LDH. When the reaction time reaches 90 min, the removal efficiencies of the two LDH are both close to 98%, respectively, which means that both two LDH can effectively remove Cr^{6+} in sufficient time.

There are several limitations in this research that is needed to deal with by future work. Firstly, as mentioned in literature review, pH is also one of the important factors affecting the efficiency of LDH adsorption of Cr^{6+}. Subsequent research will focus on exploring the changes in the adsorption properties of Mn/Al-LDH and modified Zeolite-Mn/Al-LDH for Cr^{6+} in environment of different pH values. Secondly, since the LDH material is composed of metal cations of different valence states and interlayer anions, other metal cations and anions in wastewater solution also affect the structure of the prepared material. In addition, a particularly important item in the future work is the further study of the removal mechanism. In this study, the exploration of the removal mechanism was speculative through previous studies, which was not convincing. In the future, it is necessary to continue the characterization of the LDH material after the adsorption is completed to discuss whether the adsorption mechanism of LDH material for Cr6 + in this study is consistent with the conjecture of this study. The experimental conditions applied in this study is an ideal environment, which

means that there is no interference of other metal cations and anions. In reality, there are many metal cations and other anions in the industrial wastewater containing Cr. In the future work, it is planned to study the actual industrial wastewater containing Cr as experimental materials, and explore the adsorption performance of LDH materials in different conditions to improve its application potential in industrial production.

References

1. YAO Jun, W.W.-x., YANG Xiao-duan,MA Ming-you, and L.J. ZOU Sheng-jun, ZHANG Yong-kang, *The Pollution From the Electro-manganese Plant in Wan Rong Jiang River.* Journal of Jishou University(Natural Science Edition), 1999. **20**: p. 74-77.
2. lu, L., *Research State and Progress of Textile Printing and Dyeing Wastewater Treatment Technologies.* Journal of Shanghai University of Engineering Science, 2017. **31**: p. 174-182.
3. YAO Jun, W.W.-x., YANG Xiao-duan,MA Ming-you, ZOU Sheng-jun,LIU Jun,ZHANG Yong-kang, *The Pollution From the Electro-manganese Plant in Wan Rong Jiang River.* JOURNAL OF JISHOU UNIVERSITY(NATURAL SCIENCE EDITION), 1999. **20**.
4. Xu, J., et al., *Ecological risk assessment of heavy metals in soils surrounding oil waste disposal areas.* Environmental Monitoring and Assessment, 2016. **188**(2): p. 125.
5. Briki, M., et al., *Characterization, distribution, and risk assessment of heavy metals in agricultural soil and products around mining and smelting areas of Hezhang, China.* Environmental Monitoring and Assessment, 2015. **187**(12): p. 767.
6. Li, Z., et al., *A review of soil heavy metal pollution from mines in China: Pollution and health risk assessment.* Science of The Total Environment, 2014. **468-469**: p. 843-853.

10. Baral, A. and R.D. Engelken, *Chromium-based regulations and greening in metal finishing industries in the USA.* Environmental Science & Policy, 2002. **5**(2): p. 121-133.

11. Rao, M., A.V. Parwate, and A.G. Bhole, *Removal of Cr6+ and Ni2+ from aqueous solution using bagasse and fly ash.* Waste Management, 2002. **22**(7): p. 821-830.

12. Rajput, S., C.U. Pittman, and D. Mohan, *Magnetic magnetite (Fe3O4) nanoparticle synthesis and applications for lead (Pb2+) and chromium (Cr6+) removal from water.* Journal of Colloid and Interface Science, 2016. **468**: p. 334-346.

13. Berner, T.O., M.M. Murphy, and R. Slesinski, *Determining the safety of chromium tripicolinate for addition to foods as a nutrient supplement.* Food and Chemical Toxicology, 2004. **42**(6): p. 1029-1042.

14. Hermann, J., et al., *Effects of dietary chromium, copper and zinc on plasma lipid concentrations in male Japanese quail.* Nutrition Research, 1998. **18**(6): p. 1017-1027.

15. Baruthio, F., *Toxic effects of chromium and its compounds.* Biological Trace Element Research, 1992. **32**(1): p. 145-153.

16. Tunali, S., I. Kiran, and T. Akar, *Chromium(VI) biosorption characteristics of Neurospora crassa fungal biomass.* Minerals Engineering, 2005. **18**(7): p. 681-689.

17. Sudha Bai, R. and T.E. Abraham, *Studies on chromium(VI) adsorption–*

desorption using immobilized fungal biomass. Bioresource Technology, 2003. **87**(1): p. 17-26.

18. Goyal, N., S.C. Jain, and U.C. Banerjee, *Comparative studies on the microbial adsorption of heavy metals.* Advances in Environmental Research, 2003. **7**(2): p. 311-319.

19. Prasad, M.N.V. and H. Freitas, *Removal of toxic metals from solution by leaf, stem and root phytomass of Quercus ilex L. (holly oak).* Environmental Pollution, 2000. **110**(2): p. 277-283.

20. Rives, V., Ulibarri, A.M., 1999. *Layered double hydroxides (LDH) intercalated with metal coordination compounds and oxometalates*. Coord. Chem. Rev. 181, 61–120.

21. Gu, Z., Atherton, J.J., Xu, Z.P., 2015. *Hierarchical layered double hydroxide nanocomposites: structure, synthesis and applications*. Chem. Commun. 51, 3024–3036.

22. Baral, A. and R.D. Engelken, *Chromium-based regulations and greening in metal finishing industries in the USA.* Environmental Science & Policy, 2002. **5**(2): p. 121-133.

23. Ozaki, H., K. Sharma, and W. Saktaywin, *Performance of an ultra-low-pressure reverse osmosis membrane (ULPROM) for separating heavy metal: effects of interference parameters.* Desalination, 2002. **144**(1): p. 287-294.

24. Matlock, M.M., B.S. Howerton, and D.A. Atwood, *Chemical precipitation of heavy metals from acid mine drainage.* Water Research, 2002. **36**(19): p.

4757-4764.

25. Wang, L.K., et al., *Chemical Precipitation*, in *Physicochemical Treatment Processes*, L.K. Wang, Y.-T. Hung, and N.K. Shammas, Editors. 2005, Humana Press: Totowa, NJ. p. 141-197.

26. Gerasopoulos, K., et al., *Feed supplemented with polyphenolic byproduct from olive mill wastewater processing improves the redox status in blood and tissues of piglets.* Food and Chemical Toxicology, 2015. **86**: p. 319-327.

27. Lou, J.-C. and C.-K. Chang, *Completely treating heavy metal laboratory waste liquid by an improved ferrite process.* Separation and Purification Technology, 2007. **57**(3): p. 513-518.

28. Tu, Y.-J., et al., *Treatment of complex heavy metal wastewater using a multi-staged ferrite process.* Journal of Hazardous Materials, 2012. **209-210**: p. 379-384.

29. Xin-hua, H.Y.-j.S.T.-t.X.X.-q.T.L.-s.X., *Research on Low-level Hg(II) Removal from Water by the Heavy Metal Capturing Agent.* environmental Science, 2013. **34**: p. 3487-3492.

30. Ranjan, A.T.a.M.R., *Heavy Metal Removal from Wastewater Using Low Cost Adsorbents.* Bioremediation & Biodegradation, 2015. **6**(6).

31. Ihsanullah, et al., *Heavy metal removal from aqueous solution by advanced carbon nanotubes: Critical review of adsorption applications.* Separation and Purification Technology, 2016. **157**: p. 141-161.

32. Wan Ngah, W.S., L.C. Teong, and M.A.K.M. Hanafiah, *Adsorption of dyes and heavy metal ions by chitosan composites: A review.* Carbohydrate Polymers, 2011. **83**(4): p. 1446-1456.

33. Pamukoglu, M.Y. and F. Kargi, *Removal of Cu(II) ions by biosorption onto powdered waste sludge (PWS) prior to biological treatment in an activated sludge unit: A statistical design approach.* Bioresource Technology, 2009. **100**(8): p. 2348-2354.

34. Thibault A. Guillemet , P.M., Émile Delcarte , Georges C. Lognay , Adeline Gillet, Jean-Jacques Claustriaux , Marc Culot *Factors influencing microbiological and chemical composition of South-Belgian raw sludge.* Biotechnol. Agron. Soc. Environ. , 2009. **13**: p. 249-255.

35. Rulkens, W., *Sewage Sludge as a Biomass Resource for the Production of Energy: Overview and Assessment of the Various Options.* Energy & Fuels, 2008. **22**(1): p. 9-15.

36. Foroughi, M.R. and M. Zarei, *Synthesis of hydroxyapatite nanoparticles for the removal of Pb(II) and Cd(II) from industrial wastewaters.* Research on Chemical Intermediates, 2015. **41**(6): p. 4009-4019.

37. Malaviya, P. and A. Singh, *Bioremediation of chromium solutions and chromium containing wastewaters.* Critical Reviews in Microbiology, 2016. **42**(4): p. 607-633.

38. Nancharaiah, Y.V., S. Venkata Mohan, and P.N.L. Lens, *Metals removal and recovery in bioelectrochemical systems: A review.* Bioresource Technology,

2015. **195**: p. 102-114.

39. Brahmi, K., et al., *Removal of zinc ions from synthetic and industrial Tunisian wastewater by electrocoagulation using aluminum electrodes.* Desalination and Water Treatment, 2015. **56**(10): p. 2689-2698.

40. M. A. González , R.T., I. Pavlovic , C. Barriga and F. La Mantia *Capturing Cd(II) and Pb(II) from contaminated water sources by electro-deposition on hydrotalcite-like compounds.* royal society of chemistry, 2015. **18**: p. 1838-1845.

41. Nędzarek, A., et al., *The influence of pH and BSA on the retention of selected heavy metals in the nanofiltration process using ceramic membrane.* Desalination, 2015. **369**: p. 62-67.

42. Zhang, J., M. Zhang, and K. Zhang, *Fabrication of poly(ether sulfone)/poly(zinc acrylate) ultrafiltration membrane with anti-biofouling properties.* Journal of Membrane Science, 2014. **460**: p. 18-24.

43. Qiu, Y.-R. and L.-J. Mao, *Removal of heavy metal ions from aqueous solution by ultrafiltration assisted with copolymer of maleic acid and acrylic acid.* Desalination, 2013. **329**: p. 78-85.

44. Lin, R., *ADSORPTION PROPERTIES OF AEROMONAS LOADED BY NANO-Fe3O4 ON LEAD WASTEWATER.* Southwest Jiaotong University, 2018.

45. Selvi, K., S. Pattabhi, and K. Kadirvelu, *Removal of Cr(VI) from aqueous solution by adsorption onto activated carbon.* Bioresource Technology, 2001. **80**(1): p. 87-89.

46. Nag, S., et al., *Removal of chromium(VI) from aqueous solutions using rubber leaf powder: batch and column studies.* Desalination and Water Treatment, 2016. **57**(36): p. 16927-16942.

47. Lee, S.M., et al., *Synthesis of functionalized biomaterials and its application in the efficient remediation of aquatic environment contaminated with Cr(VI).* Chemical Engineering Journal, 2016. **296**: p. 35-44.

48. Chen, C.-Y., C.-L. Chiang, and C.-R. Chen, *Removal of heavy metal ions by a chelating resin containing glycine as chelating groups.* Separation and Purification Technology, 2007. **54**(3): p. 396-403.

49. El-Bahy, S.M. and Z.M. El-Bahy, *Synthesis and characterization of a new iminodiacetate chelating resin for removal of toxic heavy metal ions from aqueous solution by batch and fixed bed column methods.* Korean Journal of Chemical Engineering, 2016. **33**(8): p. 2492-2501.

50. Darmograi, G., et al., *Study of Adsorption and Intercalation of Orange-Type Dyes into Mg–Al Layered Double Hydroxide.* The Journal of Physical Chemistry C, 2015. **119**(41): p. 23388-23397.

51. Lei, X., et al., *Activated MgAl-layered double hydroxide as solid base catalysts for the conversion of fatty acid methyl esters to monoethanolamides.* Applied Catalysis A: General, 2011. **399**(1): p. 87-92.

52. Roelofs, J.C.A.A., et al., *On the Structure of Activated Hydrotalcites as Solid Base Catalysts for Liquid-Phase Aldol Condensation.* Journal of Catalysis, 2001. **203**(1): p. 184-191.

53. Z. Matusinovic, C.A.W., *Fire retardancy and morphology of layered double hydroxide nanocomposites: a review.* J. Mater. Chem., 2012. **22**: p. 18701-18704

54. Zubair, M., et al., *Recent progress in layered double hydroxides (LDH)-containing hybrids as adsorbents for water remediation.* Applied Clay Science, 2017. **143**: p. 279-292.

55. S. He, Z.A., M. Wei, D.G. Evans, X. Duan, *Layered double hydroxide-based catalysts: nanostructure design and catalytic performance.* Chem. Commun., 2013. **49**: p. 5912-5920

56. Cavani, F., F. Trifirò, and A. Vaccari, *Hydrotalcite-type anionic clays: Preparation, properties and applications.* Catalysis Today, 1991. **11**(2): p. 173-301.

57. Vaccari, A., *Layered double hydroxides: present and future: V. Rives (Ed.), Nova Science Publishers, Inc., New York, 2001, IX+439 pp., ISBN 1-59033-060-9.* Applied Clay Science, 2002. **22**(1): p. 75-76.

58. J.L. Rendon, J.E.I., Carlos J. Serna, *Crystal-chemical study of layered [Al2Li (OH)6]+X− · nH2O.* clay clay miner, 1982. **30**: p. 180-184.

59. Bîrjega, R., et al., *Rare-earth elements modified hydrotalcites and corresponding mesoporous mixed oxides as basic solid catalysts.* Applied Catalysis A: General, 2005. **288**(1): p. 185-193.

60. Poonoosamy, J., et al., *Zr-containing layered double hydroxides: Synthesis,*

characterization, and evaluation of thermodynamic properties. Applied Clay Science, 2018. **151**: p. 54-65.

61. Velu, S., et al., *Effect of Sn Incorporation on the Thermal Transformation and Reducibility of M(II)Al-Layered Double Hydroxides [M(II) = Ni or Co].* Chemistry of Materials, 2000. **12**(3): p. 719-730.

62. D. Wang, N.G., S. Qian, J. Li, Y. Qiao, X. Liu, *Selenium doped Ni–Ti layered double hydroxide (Ni–Ti LDH) films with selective inhibition effect to cancer cells and bacteria.* RSC Adv., 2015. **5**: p. 106848-106859

63. Intissar, M., et al., *Reinvestigation of the Layered Double Hydroxide Containing Tetravalent Cations: Unambiguous Response Provided by XAS and Mössbauer Spectroscopies.* Chemistry of Materials, 2003. **15**(24): p. 4625-4632.

64. Kameda, T., H. Takeuchi, and T. Yoshioka, *Hybrid inorganic/organic composites of Mg–Al layered double hydroxides intercalated with citrate, malate, and tartrate prepared by co-precipitation.* Materials Research Bulletin, 2009. **44**(4): p. 840-845.

65. F. Leroux, C.T.-G., *Fine tuning between organic and inorganic host structure: new trends in layered double hydroxide hybrid assemblies.* J. Mater. Chem., 2005. **15**: p. 3628-3642.

66. Rives, V. and M.a. Angeles Ulibarri, *Layered double hydroxides (LDH) intercalated with metal coordination compounds and oxometalates.* Coordination Chemistry Reviews, 1999. **181**(1): p. 61-120.

67. Layrac, G., et al., *Controlled Growth of Cyano-Bridged Coordination Polymers into Layered Double Hydroxides.* The Journal of Physical Chemistry C, 2011. **115**(8): p. 3263-3271.

68. Coronado, E., et al., *Confined Growth of Cyanide-Based Magnets in Two Dimensions.* Inorganic Chemistry, 2010. **49**(4): p. 1313-1315.

69. Q. Wang, X.Z., C.J. Wang, J. Zhu, Z. Guo, D. O'Hare, *Polypropylene/layered double hydroxide nanocomposites.* J. Mater. Chem., 2012. **22**: p. 19113-19121.

70. Tian, R., et al., *Applications of Layered Double Hydroxide Materials: Recent Advances and Perspective*, in *50 Years of Structure and Bonding – The Anniversary Volume*, D.M.P. Mingos, Editor. 2017, Springer International Publishing: Cham. p. 65-84.

71. Meng, W., et al., *Preparation and intercalation chemistry of magnesium–iron(III) layered double hydroxides containing exchangeable interlayer chloride and nitrate ions.* Materials Research Bulletin, 2004. **39**(9): p. 1185-1193.

72. Yao, F., et al., *Preparation and Regulating Cell Adhesion of Anion-Exchangeable Layered Double Hydroxide Micropatterned Arrays.* ACS Applied Materials & Interfaces, 2015. **7**(7): p. 3882-3887.

73. Reichle, W.T., *Synthesis of anionic clay minerals (mixed metal hydroxides, hydrotalcite).* Solid State Ionics, 1986. **22**(1): p. 135-141.

74. Takehira, K. and T. Shishido, *Preparation of supported metal catalysts*

starting from hydrotalcites as the precursors and their improvements by adopting "memory effect". Catalysis Surveys from Asia, 2007. **11**(1): p. 1-30.

75. Marangoni, R., et al., *PVA nanocomposites reinforced with Zn2Al LDHs, intercalated with orange dyes.* Journal of Solid State Electrochemistry, 2011. **15**(2): p. 303-311.

76. Velu, S., K. Suzuki, and T. Osaki, *Selective production of hydrogen by partial oxidation of methanol over catalysts derived from CuZnAl-layered double hydroxides.* Catalysis Letters, 1999. **62**(2): p. 159-167.

77. Chang, Z., et al., *Synthesis of [Zn–Al–CO3] layered double hydroxides by a coprecipitation method under steady-state conditions.* Journal of Solid State Chemistry, 2005. **178**(9): p. 2766-2777.

78. Wang, Q., et al., *Use of Fe(II)Fe(III)-LDHs prepared by co-precipitation method in a heterogeneous-Fenton process for degradation of Methylene Blue.* Catalysis Today, 2014. **224**: p. 41-48.

79. Yang, K., et al., *Adsorptive removal of phosphate by Mg–Al and Zn–Al layered double hydroxides: Kinetics, isotherms and mechanisms.* Separation and Purification Technology, 2014. **124**: p. 36-42.

80. Chagas, L.H., et al., *MgCoAl and NiCoAl LDHs synthesized by the hydrothermal urea hydrolysis method: Structural characterization and thermal decomposition.* Materials Research Bulletin, 2015. **64**: p. 207-215.

81. Clark, I., et al., *Continuous hydrothermal synthesis of Ca2Al-NO3 layered*

double hydroxides: The impact of reactor temperature, pressure and NaOH concentration on crystal characteristics. Journal of Colloid and Interface Science, 2017. **504**: p. 492-499.

82. Wang, N., et al., *Anion-intercalated layered double hydroxides modified test strips for detection of heavy metal ions.* Talanta, 2016. **148**: p. 301-307.

83. Pavlovic, I., et al., *Adsorption of Cu2+, Cd2+ and Pb2+ ions by layered double hydroxides intercalated with the chelating agents diethylenetriaminepentaacetate and meso-2,3-dimercaptosuccinate.* Applied Clay Science, 2009. **43**(1): p. 125-129.

84. Rojas, R., et al., *EDTA modified LDHs as Cu2+ scavengers: Removal kinetics and sorbent stability.* Journal of Colloid and Interface Science, 2009. **331**(2): p. 425-431.

85. Yanming, S., Dongbin, L., Shifeng, L., Lihui, F., Shuai, C., Haque, M.A., 2013. *Removal of lead from aqueous solution on glutamate intercalated layered double hydroxide.* Arab. J. Chem.

86. Yasin, Y., Ahmad, F.B.H., Ghaffari-Moghaddam, M., Khajeh, M., 2014. *Application of a hybrid artificial neural network–genetic algorithm approach to optimize the lead ions removal from aqueous solutions using intercalated tartrate-Mg–Al layered double hydroxides.* Environ. Nanotechnol. Monit. Manag. 1–2, 2–7.

87. González, M.A., Pavlovic, I., Rojas-Delgado, R., Barriga, C., 2014. *Removal*

of Cu2 +, Pb2 + and Cd2 + by layered double hydroxide-humate hybrid. Sorbate and sorbent comparative studies. Chem. Eng. J. 254, 605–611.

88. Cao, Y., Li, G., Li, X., 2016. *Graphene/layered double hydroxide nanocomposite: properties, synthesis, and applications.* Chem. Eng. J. 292, 207–223.

89. Daud, M., Kamal, M.S., Shehzad, F., Al-Harthi, M.A., 2016. *Graphene/layered double hydroxides nanocomposites: a review of recent progress in synthesis and applications.* Carbon 104, 241–252.

90. Bi, B., Xu, L., Xu, B., Liu, X., 2011. *Heteropoly blue-intercalated layered double hydroxides for cationic dye removal from aqueous media.* Appl. Clay Sci. 54, 242–247.

91. Ma, S., Chen, Q., Li, H., Wang, P., Islam, S.M., Gu, Q., Yang, X., Kanatzidis, M.G., 2014. *Highly selective and efficient heavy metal capture with polysulfide intercalated layered double hydroxides.* J. Mater. Chem. A 2, 10280–10289.

92. Rojas, R., 2014. *Copper, lead and cadmium removal by Ca Al layered double hydroxides.* Appl. Clay Sci. 87, 254–259.

93. Bo, L., Li, Q., Wang, Y., Gao, L., Hu, X., Yang, J., 2015. *One-pot hydrothermal synthesis of thrust spherical Mg–Al layered double hydroxides/MnO2 and adsorption for Pb(II) from aqueous solutions.* J. Environ. Chem. Eng. 3, 1468–1475.

94. Zhang, H., Huang, F., Liu, D.L., Shi, P., 2015a. *Highly efficient removal of*

Cr(VI) from wastewater via adsorption with novel magnetic Fe3O4@C@MgAl-layered double- hydroxide. Chin. Chem. Lett. 26, 1137–1143.

95. Sheng, G., Hu, J., Li, H., Li, J., Huang, Y., 2016. *Enhanced sequestration of Cr(VI) by nanoscale zero-valent iron supported on layered double hydroxide by batch and XAFS study.* Chemosphere 148, 227–232.

96. Gore, C.T., Omwoma, S., Chen, W., Song, Y.F., 2016. Interweaved LDH/PAN nanocomposite films: application in the design of effective hexavalent chromium adsorption technology. Chem. Eng. J. 284, 794–801.

97. Grover, K., S. Komarneni, and H. Katsuki, *Synthetic hydrotalcite-type and hydrocalumite-type layered double hydroxides for arsenate uptake.* Applied Clay Science, 2010. **48**(4): p. 631-637.

98. Pshinko, G. N., Kosorukov, A. A., Puzyrnaya, L. N., Kobets, S. A., 2013. *Recovery of U(VI) from aqueous media with layered double hydroxides of Zn and Al, intercalated with complexones*. Radiochemistry, **55**(6): p. 601-604.

99. Hossein Beyki, M., Alijani, H., Fazli, Y., 2016. *Poly o-phenylenediamine-MgAl@CaFe2O4 nanohybrid for effective removing of lead(II), chromium(III) and anionic azo dye.* Process Saf. Environ. Prot. 102, 687–699.

100. Yue, X., Liu, W., Chen, Z., Lin, Z., 2016. *Simultaneous removal of Cu(II) and Cr(VI) by Mg–Al–Cl layered double hydroxide and mechanism insight*. J.

Environ. Sci. 1–11.

101. Yuan, X., Wang, Y., Wang, J., Zhou, C., Tang, Q., Rao, X., 2013. *Calcined graphene/MgAl- layered double hydroxides for enhanced Cr(VI) removal.* Chem. Eng. J. 221, 204–213.

102. Kameda, T., Kondo, E., Yoshioka, T., 2014. *Kinetics of Cr(VI) removal by Mg-Al layered 2+ double hydroxide doped with Fe* . J. Water Process Eng. 4, 134–136.

103. Liu, Y., Luo, C., Cui, G.J., Yan, S.Q., 2015. *Synthesis of manganese dioxide/iron oxide/ graphene oxide magnetic nanocomposites for hexavalent chromium removal.* RSC Adv. 5, 54156–54164.

104. Guo, X., Zhang, F., Peng, Q., Xu, S., Lei, X., Evans, D.G., Duan, X., 2011. *Layered double hydroxide/eggshell membrane: an inorganic biocomposite membrane as an efficient adsorbent for Cr(VI) removal.* Chem. Eng. J. 166, 81–87.

105. Tian, W., Kong, X., Jiang, M., Lei, X., Duan, X., 2016a. *Hierarchical layered double hydroxide epitaxially grown on vermiculite for Cr(VI) removal.* Mater. Lett. 175, 110–113.

106. Deng, L., Shi, Z., Wang, L., Zhou, S., 2017. *Fabrication of a novel NiFe2O4/Zn-Al layered double hydroxide intercalated with EDTA composite and its adsorption behavior for Cr(VI) from aqueous solution.* J. Phys. Chem. Solids 104, 79–90.

107. Chen, C.R., Zeng, H.Y., Xu, S., Liu, X.J., Duan, H.Z., Han, J., 2016. *Preparation*

of mesoporous material from hydrotalcite/carbon composite precursor for chromium (VI) removal. J. Taiwan Inst. Chem. Eng. 70, 302–310.

108. Lei, C., Zhu, X., Zhu, B., Jiang, C., Le, Y., Yu, J., 2016. *Superb adsorption capacity of hierarchical calcined Ni/Mg/Al layered double hydroxides for Congo red and Cr(VI) ions.* J. Hazard. Mater. 321, 801–811.

109. Ardau, C., F. Frau, and P. Lattanzi, *New data on arsenic sorption properties of Zn–Al sulphate layered double hydroxides: Influence of competition with other anions.* Applied Clay Science, 2013. **80-81**: p. 1-9.

110. Zhang, H., et al., *Highly efficient removal of Cr(VI) from wastewater via adsorption with novel magnetic Fe3O4@C@MgAl-layered double-hydroxide.* Chinese Chemical Letters, 2015. **26**(9): p. 1137-1143.

111. Chen, H., et al., *Removal process of nickel(II) by using dodecyl sulfate intercalated calcium aluminum layered double hydroxide.* Applied Clay Science, 2016. **132-133**: p. 419-424.

112. Costantino, U., et al., *New Synthetic Routes to Hydrotalcite-Like Compounds — Characterisation and Properties of the Obtained Materials.* European Journal of Inorganic Chemistry, 1998. **1998**(10): p. 1439-1446.

113. CHEN, T.L.a.F., *Atomic dipole moment corrected Hirshfeld population method.* Journal of Theoretical and Computational Chemistr, 2011. **11**: p. 163-183.

114. Zhao, J., et al., *Synthesis of one-dimensional α-Fe2O3/Bi2MoO6 heterostructures by electrospinning process with enhanced photocatalytic*

activity. Journal of Alloys and Compounds, 2015. **646**: p. 417-424.

115. Roelofs, J.C.A.A., A.J. van Dillen, and K.P. de Jong, *Base-catalyzed condensation of citral and acetone at low temperature using modified hydrotalcite catalysts.* Catalysis Today, 2000. **60**(3): p. 297-303.

116. Lowell, S. et al., *Surface Area Analysis from the Langmuir and BET Theories*. Characterization of Porous Solids and Powders: Surface Area, Pore Size and Density, 2004. **16**: p. 58-81.

117. Carriazo, D.; Del Arco, M.; Martin, C.; Rives, V. *A comparative study between chloride and calcined carbonate hydrotalcites as adsorbents for Cr(VI).* Appl. Clay Sci. 2007, **37**, 231-239.

118. Zhu, K. et al., *Polyaniline-Modified Mg/Al Layered Double Hydroxide Composites and Their Application in Efficient Removal of Cr(VI).* ACS Sustainable Chemistry & Engineering, 2016. 4: **p**. 4361-4369.

119. He, X., Qiu, X. H., Chen, J. Y., *Preparation of Fe(II)–Al layered double hydroxides: Application to the adsorption/reduction of chromium.* Colloids and Surfaces A: Physicochemical and Engineering Aspects, 2017. **516**: p. 362-374.